NASA/TM–2012-217513

The Ocean Radiometer for Carbon Assessment (ORCA): Optical Design and Performance

Mark Wilson, Alan Holmes, Charles McClain, Gerhard Meister, Bryan Monosmith, Manuel Quijada, James Smith, Eugene Waluschka

National Aeronautics and
Space Administration

Goddard Space Flight Center
Greenbelt, Maryland 20771

July 2013

AVAILABLE ONLY WITH APPROVAL OF
Goddard Space Flight Center, Greenbelt, MD 20771

NASA STI Program ... in Profile

Since its founding, NASA has been dedicated to the advancement of aeronautics and space science. The NASA scientific and technical information (STI) program plays a key part in helping NASA maintain this important role.

The NASA STI program operates under the auspices of the Agency Chief Information Officer. It collects, organizes, provides for archiving, and disseminates NASA's STI. The NASA STI program provides access to the NASA Aeronautics and Space Database and its public interface, the NASA Technical Report Server, thus providing one of the largest collections of aeronautical and space science STI in the world. Results are published in both non-NASA channels and by NASA in the NASA STI Report Series, which includes the following report types:

- TECHNICAL PUBLICATION. Reports of completed research or a major significant phase of research that present the results of NASA Programs and include extensive data or theoretical analysis. Includes compilations of significant scientific and technical data and information deemed to be of continuing reference value. NASA counterpart of peer-reviewed formal professional papers but has less stringent limitations on manuscript length and extent of graphic presentations.
- TECHNICAL MEMORANDUM. Scientific and technical findings that are preliminary or of specialized interest, e.g., quick release reports, working papers, and bibliographies that contain minimal annotation. Does not contain extensive analysis.
- CONTRACTOR REPORT. Scientific and technical findings by NASA-sponsored contractors and grantees.
- CONFERENCE PUBLICATION. Collected papers from scientific and technical conferences, symposia, seminars, or other meetings sponsored or co-sponsored by NASA.
- SPECIAL PUBLICATION. Scientific, technical, or historical information from NASA programs, projects, and missions, often concerned with subjects having substantial public interest.
- TECHNICAL TRANSLATION. English-language translations of foreign scientific and technical material pertinent to NASA's mission.

Specialized services also include organizing and publishing research results, distributing specialized research announcements and feeds, providing help desk and personal search support, and enabling data exchange services. For more information about the NASA STI program, see the following:

- Access the NASA STI program home page at http://www.sti.nasa.gov
- E-mail your question via the Internet to help@sti.nasa.gov
- Fax your question to the NASA STI Help Desk at 443-757-5803
- Phone the NASA STI Help Desk at 443-757-5802
- Write to:

  NASA STI Help Desk
  NASA Center for AeroSpace Information
  7115 Standard Drive
  Hanover, MD 21076-1320

AVAILABLE ONLY WITH APPROVAL OF
Goddard Space Flight Center, Greenbelt, MD 20771

NASA/TM–2013-217513

The Ocean Radiometer for Carbon Assessment (ORCA): Optical Design and Performance

Mark Wilson
NASA's Goddard Space Flight Center, Greenbelt, MD

Alan Holmes
Santa Barbara Instrument Group Santa Barbara, CA

Charles McClain
NASA's Goddard Space Flight Center, Greenbelt, MD

Gerhard Meister
NASA's Goddard Space Flight Center, Greenbelt, MD

Bryan Monosmith
NASA's Goddard Space Flight Center, Greenbelt, MD

Manuel Quijada
NASA's Goddard Space Flight Center, Greenbelt, MD

James Smith
NASA's Goddard Space Flight Center, Greenbelt, MD

Eugene Waluschka
NASA's Goddard Space Flight Center, Greenbelt, MD

National Aeronautics and
Space Administration

Goddard Space Flight Center
Greenbelt, Maryland 20771

July 2013

AVAILABLE ONLY WITH APPROVAL OF
Goddard Space Flight Center, Greenbelt, MD 20771

Do not release on a public Web site.

AVAILABLE ONLY WITH APPROVAL OF
Goddard Space Flight Center, Greenbelt, MD 20771

Contents

Introduction

The purpose of this document is to describe the fundamental optical design of ORCA, along with some considerations and trades made in arriving at the current state of the design as implemented in the prototype instrument built under ESTO's Instrument Incubator Program from 2010-2014. A brief description of the science and system engineering requirements is given; for the purpose of this design, those requirements evolved from the original enhanced multispectral Sea-viewing Wide Field-of-view Sensor (SeaWiFS) recommended by McClain et al., 2002) to the hyperspectral Ocean Ecology Sensor recommended by the Aerosol, Cloud, and Ecology (ACE) science working group and the PACE Science Definition Team (SDT) . McClain et al. (2012) provide a detailed history of the ORCA development history, science requirements, and design overview.

Summary

The scientific purpose of the ORCA instrument is to make accurate radiometric measurements of the ocean from space. In this type of measurement, there is no need for high spatial resolution (1 km requirement), but there is a need for a large spectral range, hyperspectral resolution (5 nm) in the UV-NIR, and high signal to noise ratios, e.g., at least 1000:1 in the UV-visible. Whole earth coverage in a short time with minimal coverage gaps is required, e.g., 2-day global coverage. Minimal sensitivity of the instrument response to the state of polarization of the input beam is also required as is high image quality, e.g., minimal striping. The details of the performance requirements are outlined in Meister, et al., (2011).

The type of instrument that describes ORCA is a hyperspectral imaging spectrograph. To achieve a large field of regard, a rotating telescope is used, similar to those of SeaWiFS and the Visible Infrared Imaging Radiometer Suite (VIIRS); the telescope rotates perpendicular to the velocity vector of the spacecraft. The high signal to noise ratios (SNR) are achieved by incorporating a time delay integration (TDI) mode into the detectors, so that the signal builds up as the charge is transferred across the array. The physical pixels of the detector array are binned into sets of 8x8; this binned pixel set is called a superpixel. Each superpixel is aggregated in the TDI readout direction, increasing the SNR of the instrument (Monosmith and McClain, 2012). The wavelength range covered by ORCA is from the UV (~340 nm) up to the SWIR (2130 nm). A large number of spectral bands are created using conventional diffraction gratings in the UV & visible part of the spectrum. Currently there are 26 distinct spectral bands identified by the ACE and PACE ocean teams as necessary for biology applications and atmospheric corrections. There are 3 SWIR bands in the ORCA brass board developed under the NASA Instrument Incubator Program, but three additional SWIR bands have been recommended by the PACE SDT, each being separated using a dichroic beam splitter and a narrowband filter.

Background

ORCA can be described as a hyperspectral SeaWIFS. The major advance is adding many additional wavelength bands. To this end, some of the features of SeaWIFS have been incorporated into this design, e.g., the rotating telescope and the TDI. Many different options for the spectrograph section of ORCA have been considered over the years (e.g. prism-based dispersion, reflective camera optics, the number of TDI elements), and the final result of all the tradeoffs are described in this document. The original design concept was to use discrete

detector arrays like SeaWiFS, but as the number of required bands increased, the design evolved to a pair of spectrographs to simplify the design, maintain throughput, and minimize the instrument volume and weight.

Design Approach

The design approach was to use SeaWIFS (Barnes et al., 1994a, Barnes et al., 1994b, McClain et al., 2004) as a baseline concept, with a rotating telescope with fixed imaging optics and detector TDI techniques. A depolarizer is part of the telescope optical subsystem. The spectrograph imaging approach was to baseline flat gratings and other conventional optics as a manner of reducing risk in the manufacturing and alignment aspects of the instrument. An overall strategy was to avoid new technologies that required development or did not have flight heritage. During the optical design process, the goal was to minimize geometric blur into a single pixel or two (worst case) over all the wavelengths and the full field of view in order to meet the spectral resolution requirements. If successful, the design meets the most challenging requirements; any subsequent instrument requirements should not present any serious challenges.

Requirements

The science and systems engineering requirements imposed on the ORCA optics are in Table 1. The specific wavelength bands are in Table 2.
Below is a brief listing of these requirements:

Table 1. System Engineering Requirements for ORCA

Field of regard	+/- 58 deg
SNR (ORCA team defined; higher than ACE & PACE requirements)	~1500 in the visible
Viewing slant angle or tilt (relative to nadir)	20°
Orbital altitude	650 km
Ground resolution (along sub satellite track)	1 km
Wavelength range	342 nm – 2150 nm
Spectral resolution	5 nm/superpixel
Detector pixel size	26 micrometers (square)
Superpixel	8x8 pixels
TDI factor	16

Table 2. ORCA Band Requirements and SNR Goals (McClain et al., 2012)

Wavelength (nm)	Bandwidth (nm)	SNR (req't)	SeaWiFS SNR	Ltyp $W/(m^2\ \mu m\ sr)$	Lmax $W/(m^2\ \mu m\ sr)$
BLUE CHANNEL					
350	15	300		74.6	356
360	15	1125		72.2	376
385	15	1500		61.1	381
412	15	1500	897	78.6	602

425	15	1500		69.5	585
443	15	1500	967	70.2	664
460	15	1500		68.3	724
475	15	1500		61.9	722
490	15	1500	1010	53.1	686
510	15	1500	1000	45.8	663
532	15	1500		39.2	651
555	15	1500	870	33.9	643
RED CHANNEL					
583	15	1500		38.1	624
617	15	1500		21.9	582
640	10	1500		19.0	564
655	15	1500		16.7	535
665	10	1500	570	16.0	536
678	10	1500		14.5	519
710	15	1500		11.9	489
748	10	600	1000	9.3	447
765	40	600	522	8.3	430
820	15	600		5.9	393
865	40	600	364	4.5	333
SWIR BANDS					
1245	20	300		0.88	158
1640	40	180		0.29	82
2130	50	100		0.08	22

Radiances in W/m^2 str µm ; * is optional band used for atmospheric corrections

A comparison of predicted ORCA (flight model) SNR values versus MODIS and SeaWIFS is shown in Figure 1 below (McClain et al., 2012). The ORCA SNR values are subject to revision as more accurate information on optical components, detector and electronics performances are updated. Shown in Figure 2A is a visualization of the on orbit operations.

Figure 1 SNR Requirements, compared to MODIS and SeaWIFS

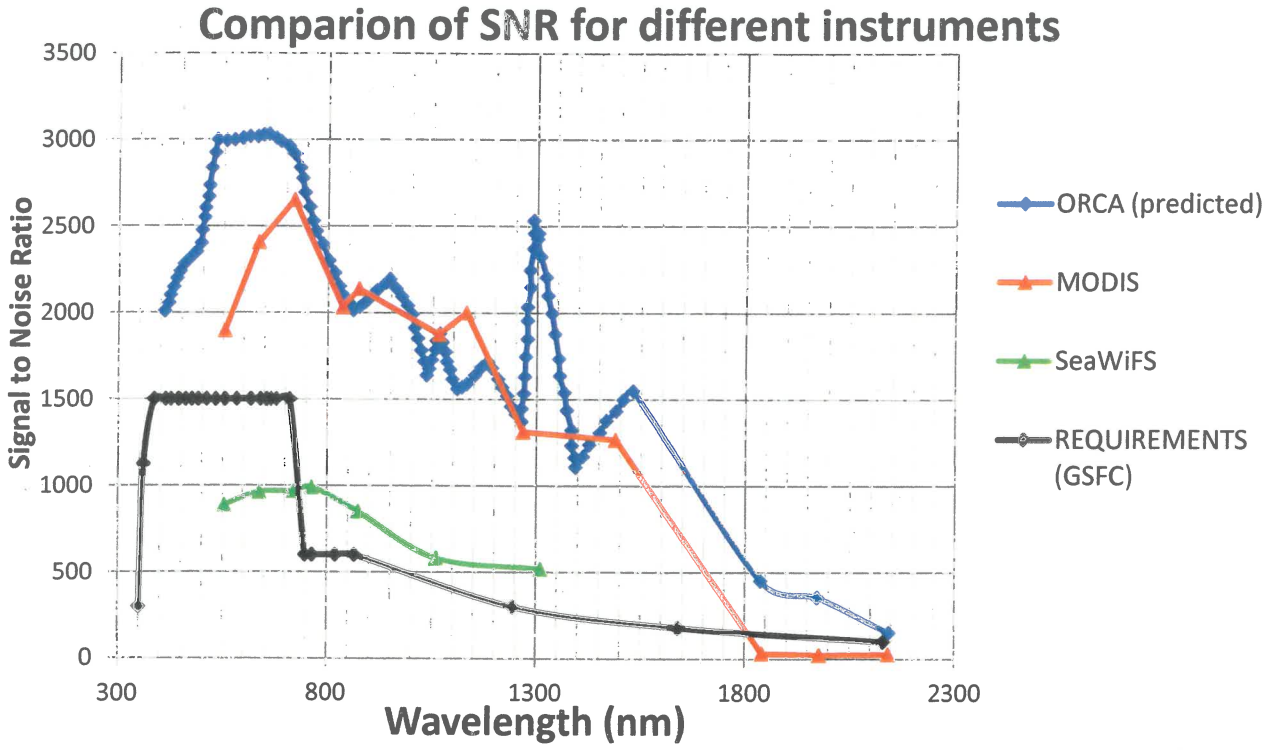

Figure 2. Orbital operations

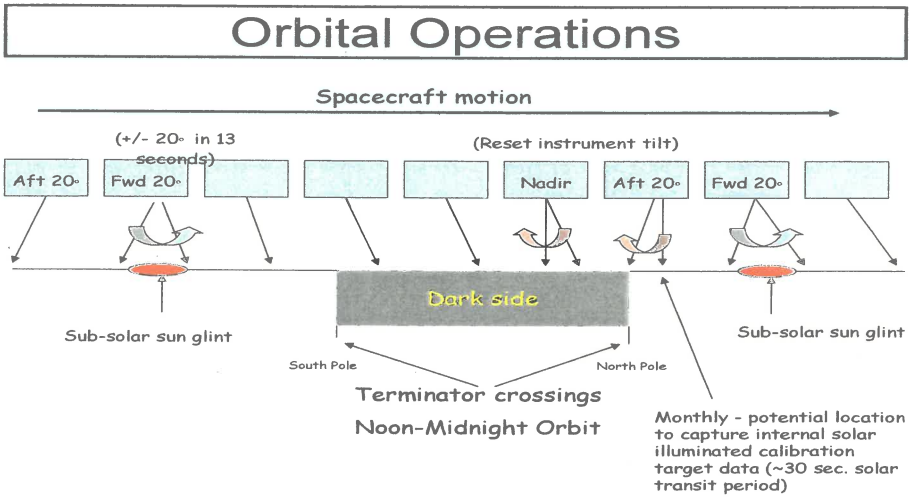

System engineering requirements and derived optical requirements

The basic function of the ORCA optical system is to image a single instantaneous field of view (IFOV) ground footprint into a single superpixel on the detector. This is true for both the spectral (longtrack) and spatial (crosstrack) directions. The sensor is tilted ±20° relative to nadir, in order to minimize sun glint off the ocean surface with the sensor viewing away from the sun. Thus, near the subsolar point, a tilt change is made so as to avoid a systematic gap in coverage at the subsolar point (Gregg and Patt, 1994). See Figure 2 for a figure showing the basic geometry of the system operations.

To calculate the parameters used in designing an optical system, such as aperture, field of view (FOV), and focal length, one uses the mapping requirement (1 ground pixel to 1 superpixel at the given spacecraft altitude) to calculate the effective focal length of the optical system. The FOV in the long track direction is just the angular size of the ground footprint; the FOV in the crosstrack direction is the long track FOV multiplied by the TDI. For these calculations, the Earth is assumed flat. There are slight distortions involved in projecting a square detector pixel onto the ground at 20° due to the slight differences in angle from one side to the other (one side of the footprint is at 20°+IFOV, the other at 20°-IFOV), but this is only a few meters on the ground and is ignored here. This affects the crosstrack ground size in a similar fashion.

Specific equations used for calculating the values used in the design are:

1) EFL = superpixel size/(crosstrack footprint/(orbital altitude/cos(spacecraft tilt))) where EFL is effective focal length.
2) FOV (spectral) = superpixel size/EFL
3) FOV (spatial) = FOV(spectral)*TDI
4) From calculations of the SNR, one can derive the collecting diameter needed to meet the requirements.

The spreadsheet used in deriving the values in the design is shown in Figure 3.

Figure 3. Spreadsheet used for ORCA optical design quantities

Diameter	90.0	mm
EFL	300.0	mm
f/no	3.3	
Altitude	650.0	km
Slant angle (y)	20.0	deg
Eff. Alt	691.7	km
Slant angle (x)	58.0	deg
Footprint	1000.0	(cross track, full width, m)
	1128.0	(along track,full width, m)
TDI ratio	16.0	
Pixel size	26.0	microns
Superpixel	8.0	pixels
FOV (x)	0.747489	half field (deg), cross track
FOV (y)	0.043901	half field (deg), long track
Slit width (x)	7.827685	(full width, mm)
Slit height (y)	0.459726	(full heighth, mm)
Superpixel size	0.208	mm
Magnification	0.452443	
EFL(sys)	135.7	
F/no (sys)	1.5	

Defined at nadir

Input Data in BLUE

includes 6% factor increase due to curvature of Earth

NOTE: THESE ARE ALL PARAXIAL OPTICAL QUANTITES (EFL, et

f/no is the f number (also shown as F/no. The "blur factor" refers to the fraction of a pixel allowed for image blur (i.e. it is related to the full width half max spread of a PSF).
During the initial phases of designing ORCA, the team conducted a tradeoff study between the size of the collecting aperture, the number of pixels in the TDI direction, and the number of pixels binned to form a superpixel. In this tradeoff, aperture sizes ranged from 70 mm to around 150 mm and the TDI factor ranged from 8 to 32. The number of pixels forming a superpixel ranged from 8 to 12. The limiting factors involved were:

a) For the primary mirror, getting a reasonable packaging size for the instrument and adequate imaging performance were the primary factors in limiting the diameter.
b) For typical apertures and pixel sizes, the system f/no was around f/1.5, which was deemed the limit at which good imaging could be achieved – this is mostly a limit of how close the detector can be to the imaging optics.
c) "Good" imaging (spot diameters ≤ 2 pixels) was required over the full FOV and bandpass of a given spectral channel. With large TDI values, this became difficult to achieve with all reflective spectrograph optics. Refractive solutions were found that could accommodate a larger TDI value. The main problem from an optical design perspective is a design with large aperture and large TDI values Large TDI values mean a larger IFOV, and with most refractive lens solutions using vary steep curvatures, so the probability of vignetting within the lens increases, as well as larger blur sizes on the focal plane.
d) The number of CCD channels or spectrographs varied as well – there were 2 initially, then 3, then back to 2. The ability to read out all the data in a sufficiently short clock cycle imposed limitations on the type of detector used and the number of bands.
e) From an optics perspective, having either a large number of pixels binned into a superpixel or a larger physical pixel is preferred – the larger the linear size of the superpixel, the larger the EFL of the system. This case means a larger f/no, making it easier to meet the image quality specs and have sufficient back focus distance that the detectors are mounted without interference between the lens structure and the detector structure. This caused issues for the detectors, because either large physical pixels were unattainable or they could not handle the data rates involved in binning more pixels.

Functional design

Figure 4 shows the functional layout of the ORCA optical system. A telescope subsystem rotates continuously 360° in the crosstrack direction. The telescope consists of a baffled tube. This subsystem consists of a primary collecting mirror and a depolarizer which are rotated together, a half angle mirror which rotates at half the rate of the telescope (in the same direction), and a (nonrotating) slit located at the image location formed by the primary mirror. The beam is collimated and sent through an internal aperture stop. The internal stop minimizes stray light going into the spectrograph optics and SWIR optics; the idea is to avoid seeing any structure from around the half angle mirror. The short wavelength light (340-565 nm) light is reflected from the front surface of a dichroic beamsplitter. This reflected light enters the blue channel optics, consisting of a diffraction grating and a focusing lens, to the first CCD in the system. Of the light that is transmitted through the blue dichroic, light from 575-880 nm is reflected into the red channel optics, also consisting of a diffraction grating and a lens

subsystem, and collected on a second CCD. Light above 880 nm is collected in three different channels using two dichroic beamsplitters. Each SWIR configuration consists of a two-element focusing lens, a narrowband filter, and a SWIR linear detector array.

Figure 4. ORCA functional optical layout

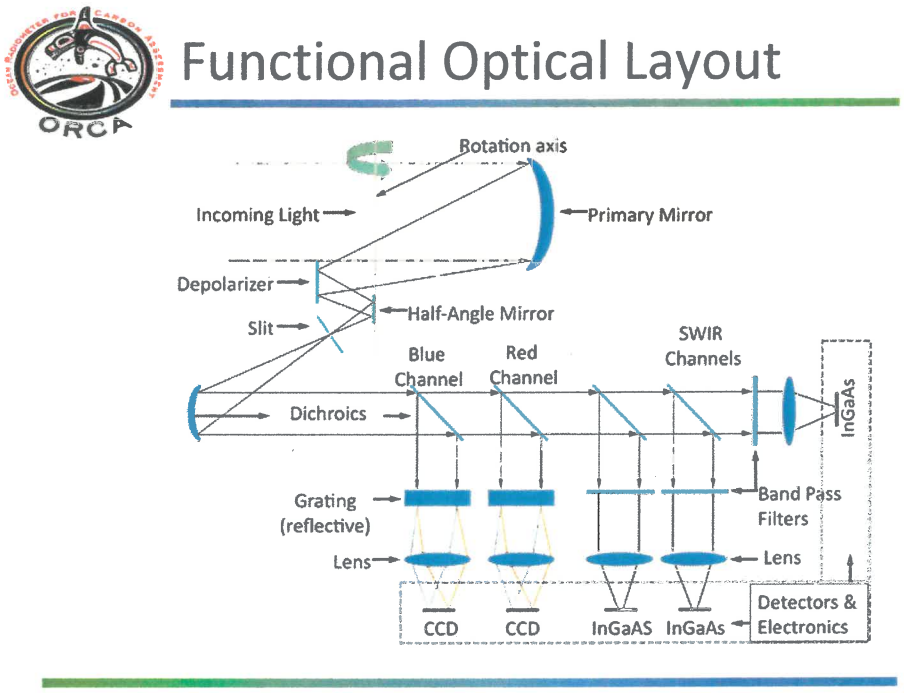

A stylized representation of the TDI technique used by ORCA is shown in Figure 5. As the scan mirror rotates, the motion of the projected ground scene on the CCD array is precisely matched by the column charge transfer rate (the rate at which photoelectrons are shifted towards the accumulation and readout registers). Effective integration times are long, equal to the time it takes to transfer charge across the entire array, and SNRs are very high. Every ground element is sampled by the same detector elements, spatially and spectrally, virtually eliminating striping. A small portion of the ORCA array is illustrated. The relationship between the slit images, the pixels, and the wavelengths are shown in Figure 6.

Figure 5

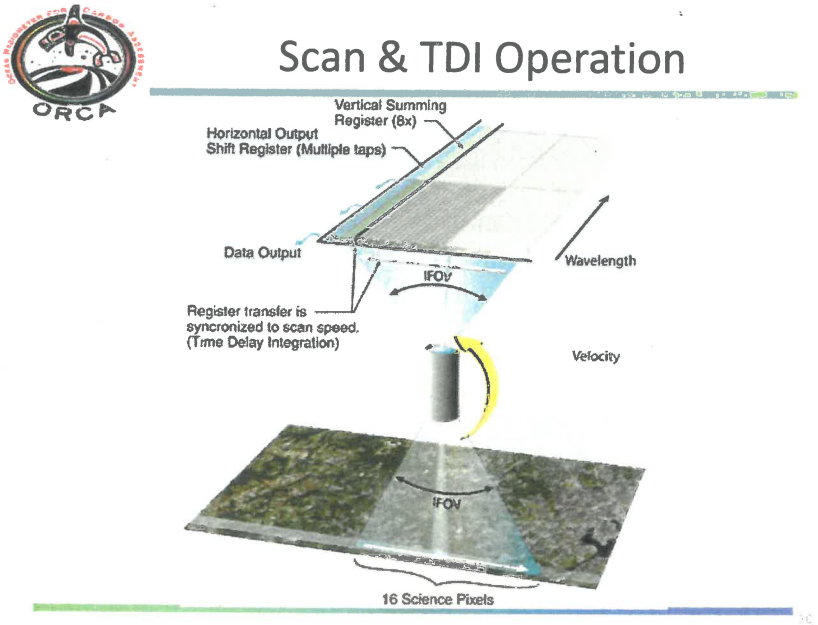

Figure 6 Detector layout - relationship of slit image to pixels

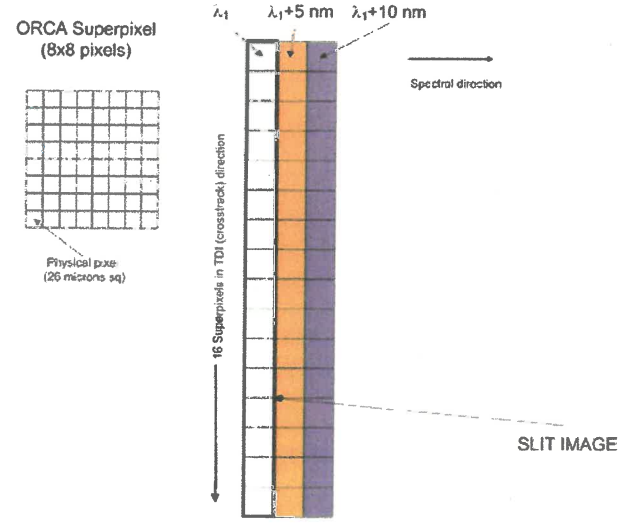

Optical design philosophy

The basic approach was to select the design that would meet all the performance specifications, but not incorporate components requiring technology development, i.e., use components and technologies that had flight heritage, to minimize risk. A constraint on actual component specifications was the amount of money available under the Instrument Incubator Program (IIP). Another important consideration was to make the design as robust or flightlike as possible, to address as many design and calibration/characterization issues as possible, thus avoiding unforeseen problems during a flight instrument build, i.e., reduce risk to cost and schedule as much as possible. Thus, the design minimized the number of mechanisms, e.g., a focus mechanism.

To this end we selected the design for the highest spacecraft altitude under consideration by the ACE mission working group (800km?), the maximum aperture needed to meet SNR requirements, and full spectral coverage,.

Rotating telescope options

There were two basic options for the telescope: 1) either a SeaWIFS-type design, with a single powered collecting optic, reflective depolarizer, and half angle mirror, or 2) a multiple mirror design. The latter would be designed to minimize the aberrations coming into the spectrograph optics, which in principle would make the spectrograph optics easier to design and could also simplify testing.

Option 1 was selected based on minimizing the mass of the telescope (speeds of up to 8 Hz have been mentioned for the rotation speed and it is preferable to have a minimum mass being rotated), and the belief that correction of the telescope aberrations could be done in the spectrograph as long as the aberrations did not vary as the telescope rotated. The chosen design looks very much like a SeaWIFS telescope design. One additional (mechanical) component added to ORCA was a slit at the best image surface of the telescope. This slit is used to improve spectral resolution and reduce stray light effects.

Telescope Optics

a. Primary mirror

In order to minimize the aberrations across the FOV, the powered mirror was changed from an off-axis parabola (OAP) to an off-axis ellipse (OAE). The collecting aperture determined from the SNR tradeoff studies was set at 90 mm diameter. The focal length of the mirror was a free design parameter. With a final system f/no of 1.5, and a general rule of thumb used in optical design being to keep (de)magnifications around a factor of two or less (the telescope would have a f/no of 3.33) for aberration correction, the focal length of the mirror would be 300 mm to keep the telescope length minimized while still being able to incorporate a depolarizer with a reflective back side and half angle mirror. See Figure 7 for a ray trace drawing of the telescope. Figure 12 shows the spot diagrams at the focal surface of the telescope.

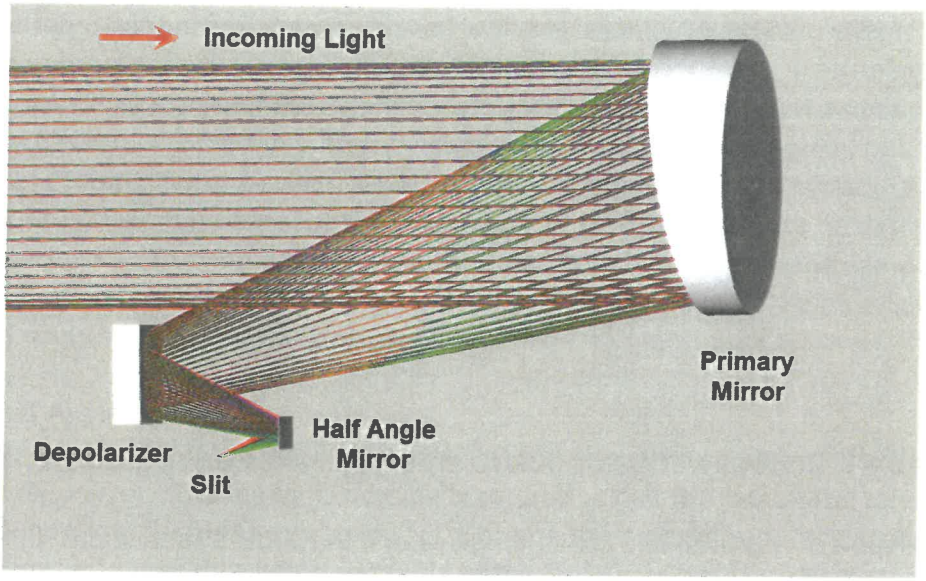

Figure 7 Ray Trace Drawing of Telescope

A magnification of 1 could be useful from a spectrograph optics point of view (e.g. one could use an Offner spectrograph), but makes the telescope focal length too short to be practical.

It is worth noting that the actual aperture stop is located further downstream in the optical train (after the collimating mirror), so the beam moves around on the primary mirror, as a function of the field of view. This aperture location is at the image of the primary mirror.

With the selection of a single powered mirror, the dominant aberrations are third-order astigmatism and field curvature, assuming the conic constant was optimized to minimize spherical aberration. The astigmatism is a function of the square of the IFOV, the field curvature depends only on the focal length of the primary mirror. Both of these aberrations must be corrected by the spectrograph optics. There also exists a small amount of distortion, which shows up as slit curvature in the cross track direction; the amount was small enough to be neglected. Coma is present near the center portion of the IFOV at the slit plane but is neglible in the detector plane.

b. Depolarizer

Patterned after the SeaWIFS depolarizer, the ORCA depolarizer is a duel wedge design with birefringent material and the crystal axes of the 2 pieces are at 45 degrees with respect to each other. Figure 7 shows a double wedge depolarizer. When the beam hits the double wedge depolarizer whose crystal axes are at 45 deg to each other, there is a variable retardance across the beam, resulting in a polarized beam becoming effectively depolarized. The wedged depolarizer works well with both monochromatic and broadband light, with the effectiveness of the depolarizer increasing with the size of the beam's cross-section. The larger the beam diameter on the depolarizer, the more effective the depolarizer becomes. In addition, use of a second piece of the same material but oriented at 180 deg with respect to the first piece minimizes the beam deviation over the full bandpass. The thickness of the depolarizer is generally determined by other optomechanical criteria (e.g. flatness of the faces), but increasing the thickness increases the amount of depolarization. For this specific design, the

depolarizer consists of two pieces of magnesium fluoride atomically bonded together. The internal wedge angle in the current design is 1.5°. A reflective coating is placed on the rear surface of the depolarizer, so the beam travels through this optic twice (see Figure 7).

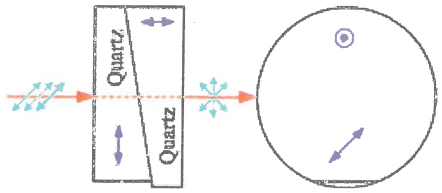

Figure 8 Double wedge depolarizer, crystal axes orientation at 45°

Because the depolarizer is used in a converging beam, it introduces aberrations, primarily focus and spherical aberration, with some additional astigmatism also introduced. The conic constant of the OAE compensates for the spherical aberration; the focus is set at the best image location.

The depolarizer causes image splitting to occur; this is due to the difference between the ordinary and extraordinary indices of refraction. Optical modeling predicts four images are created, but only two have significant energy. These different images can be seen at the slit, but are demagnified by the spectrograph optics and the spatial difference between them is smaller than the detector pixel and are not detectable.

Magnesium fluoride was chosen to be the substrate material. This was in part based on the SeaWiFS design heritage, and in part based on high transmission in the wavelength region around 320 nm, part of the original specifications for ORCA. Another alternative is to use IR grade fused silica as a substrate. Use of magnesium fluoride also reduces (slightly) both the aberrations in the telescope system and the ghost reflection from the front surface of the depolarizer compared to quartz. When light enters the telescope at an off-axis angle, the ghost reflection still lands on the detector active area in both channels, constituting a source of off-axis stray light. There are two approaches to dealing with this ghost reflection: 1) tilt the front surface of the depolarizer (relative to the rear surface of the entire depolarizer), or 2) find a coating of some kind that can be applied to the front surface in order to reduce the intensity of the ghost. Option 1 is similar to that used for SeaWIFS, would be the primary method used in ORCA, and is the easiest to physically accomplish. In this instance, the ghosts actually get directed toward the slit, and are imaged onto the detector in such a way that they coincide with the primary beam. The ghosts are always there, but the energy contributes to the measured signal for that ground pixel with some degradation of the point spread function or image quality. With respect to Option 2, it is not easy to design a multilayer dielectric coating stack to reduce the intensity of the ghosts to a very small level over the entire range of wavelengths seen by ORCA. Currently NASA has an SBIR to evaluate the feasibility of putting a so-called "moths eye" coating on the front surface which is an alternative type of coating. This is actually a nanostructure and is fabricated directly into the substrate. Such a structure has the potential to significantly reduce the intensity of the ghost, e.g., by an order of magnitude or more.

The depolarizer in ORCA has a reflective surface on the back side of the assembled optic. This usually involves putting an adhesive layer onto the glass substrate, so that the reflective coating

(such as aluminum) will adhere to the surface. In the case of ORCA, a proprietary coating of protected silver is used, so the actual adherence material is unknown.
The physical piece in the current design is square, since the beam footprint on the front surface is nearly square when considering both the beam going in and the beam going out. The piece could be either rectangular or circular. Making it circular allows a means of controlling the polarization of the system by allowing the orientation of the depolarizer to be easily adjusted to optimize performance. The depolarizer crystal axis needs to be aligned in the same direction as the grating rulings in the red and blue channels. However this enlarges the physical diameter of the optic and could introduce packaging problems.

c. Half Angle Mirror

The half angle mirror (HAM) is a flat mirror with, ideally, the same coating and surface figure on both sides of the mirror. The mirror is nominally rotated at half the rate of the telescope. For a 360 degree revolution, the HAM rotates by 180°, but on the next rotation, the second side of the mirror comes into use; thereafter each side of the HAM gets used on alternate revolutions. The rotation axis of the telescope is located at the front (reflecting) surface of the primary mirror. The rotation axis of the HAM should be the same axis. The actual reflecting surface is in front of the rotation axis by a distance equal to half the mirror thickness; this introduces a defocus effect at the ends of the field of view, so minimizing the mirror thickness minimizes the focus error.
The size of the HAM is longer in the spatial direction, by the cosine of the maximum (half) angle of the field of regard. For fabrication purposes, this angle was assumed to be 45°.

Slit

The slit is used to restrict the field of view entering the spectrograph and is located at the best focus position on axis for the telescope over the FOV. There is a tilt on the slit, relative to the chief ray at 633 nm, due to the curvature of the focal surface; this curvature is the Petzval curvature introduced by the primary mirror. Compared with most slits used in astronomical instruments, this slit aperture is quite wide, about 0.650 mm wide x 6 mm long. The front and back surfaces of the slit are flat. See Figure 8 for a picture of the slit. The optics in the spectrograph image this slit onto the detector arrays.

Figure 9 Slit Aperture

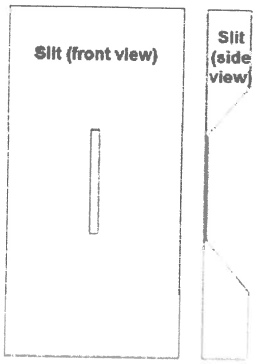

Since the index of refraction of the depolarizer varies as a function of wavelength and polarization, there are residual focus effects. The birefringent nature of the depolarizer causes separation of the two images for the s and p polarization components. This separation can be seen at the slit. The spectrograph optics demagnifies the slit image to match the superpixel size, with the result that the image separation is smaller than one detector pixel and is not detected.

Collimator

Once the tradeoff studies demonstrated a need to collimate the beam, the optic chosen was an off-axis parabola. The focal length for this mirror is a free design parameter. The longer the focal length, the larger the beam diameter of the outgoing beam but the smaller the angular divergence (from the off-axis fields). There was not a defined length of the optical system, but allowing for a large distance dictated keeping the angular divergence small. It was also desirable to allow room for a small fold mirror between the slit and collimator, for situations where it was desirable to rotate about an axis perpendicular to gravity; the nominal axis of rotation is parallel to gravity.
The solution chosen was a focal length of 100 mm. This gave an outgoing beam diameter of 30 mm, with the overall beam divergence (about 2°) such that many of the optics in the spectrograph channels would be 5-10 cm, which is within normal sizes of production by many optical fabrication companies, allowing costs to be reasonable.

Spectrograph optics

Each of the spectrograph channels consisted of the same types of optical elements: a dichroic beamsplitter, a diffraction grating, and a multielement lens system to focus the beam onto the detector. For ease of fabrication reasons, fused silica was selected as the beamsplitter substrate material; no other materials were considered for the IIP. All dichroics are set to a nominal angle of incidence of 45° for mechanical and thermal reasons. A 30° angle of incidence gives better polarization sensitivity performance but will be considered during the next phase of the project. To simplify mounting and fabrication of the gratings, the substrates were selected to be the same size and material (fused silica).

To keep all the optical elements to a practical limit and reach optimum image quality, the spectrograph optics was moved toward the collimator as close as they could get. This meant cutting an area of the optical bench so that the blue and red spectrograph channels actually went through the bench. The dichroics reflect the shortest wavelength band and transmit the longer wavelengths. The best way to implement the 2 channels, in terms of mechanical packaging, was to reflect the blue channel wavelengths in one direction perpendicular to gravity, and reflect the red channel wavelengths in the opposite direction (still perpendicular to gravity), and transmit the SWIR wavelengths. This complicates a thermal desire that the detector boards be on the same side of the instrument.

Below is a discussion of each of the spectrograph channels and the details of each channel.

a. **Blue channel spectrograph**

i. Dichroic beamsplitter – the specifications for the transmission and reflectivity requirements over the spectral range of ORCA are shown in Table 2.

Table 2. Optical specifications for blue channel dichroic:

1. Average % Reflectance > 95% (Between 345-565 nm)
2. Average % Transmission > 95% (Between 595-2160 nm)
3. Transition width from 5% to 90%: Transmission ave: 20 nm on either side of pass band

Shown in a separate document[4] are the blue band dichroic reflection and transmission curves along with the surface figure specifications. The figure specifications were determined from characteristics of good fabrication practices. Nominally the dichroic is flat, with no wedge ang between the front and rear surfaces, since ray tracing indicated that the wedge angle made no difference on light that reflected off the rear surface and double passing through the dichroic getting into the blue focusing lens. The selection of the 0° wedge angle option was made because typical substrates have no wedge angle, saving time and expense of creating the wedge angle.

ii. **Diffraction grating**

The final grating line spacing was determined using Zemax optimization, with the light in first-order being used. The angle of diffraction was intentionally kept small, using a larger angle of incidence (30°). This configuration prohibited light at zero-order from entering the lens assembly directly. There is a fair amount of energy in both the zero and -1 order so keeping that light from entering the focusing lens is important. The gratings were chosen to be flat primarily to make manufacturing easier and minimize scatter. Powered gratings are difficult to blaze properly across the full aperture of the grating.

The formula for calculating the grating space is shown below:

$m / (\sigma \cos \beta) * EFL_{lens} = \Delta S$, where ΔS is the distance on the detector between the centroids of the maximum and minimum wavelengths.

For the blue channel, the minimum wavelength was 342.5 nm, the highest is 562.5 nm, so the bandpass = 220 nm. At 5 nm per -superpixel resolution, this converts to a distance of 44 superpixels in the spectral direction, or 9.152 mm. This is the distance between the peaks of the longest and shortest wavelengths (NOT the full width-half maximum separation or FWHM). This insures that each pixel has the maximum intensity.

To achieve a FWHM for a slit image (LSF) of 5 nm per 8 pixels requires that the slit image size be 7 pixels, rather than 8. The number of pixels between

the center of the slit images for wavelengths that are 5 nm apart is still 8 pixels. The idea would be to adjust the slit image size by either reducing the slit width itself (losing energy) or adjust the angles of incidence and diffraction. Changing the angles effects the dispersion, so the grating spacing would be adjusted as needed.

The effective slit image size, for an aberration free system, on the detector, is a product of two values: the (de)magnification of the lens system, and the (de)magnification of the grating. The grating magnification (ratio of the outgoing beam diameter in the spectral plane to the incoming beam diameter) is shown in the following equation:

$$\frac{|d\beta|}{|d\alpha|} = \frac{\cos\alpha}{\cos\beta} = \frac{d_1}{d_2}$$

Where α is the angle of incidence of the beam on the grating and β is the angle of diffraction and d_1 and d_2 represent the diameters of the incident beam and diffracted beam, respectively. Note that for small diffractive angles, the beam is demagnified.

The equation for spectral dispersion, though, is only dependent on the diffractive angle:

$$\frac{d\beta}{d\lambda} = \frac{m}{\sigma\cos\beta}$$

Where σ is the groove spacing and m the order number (1 for ORCA). This means that changing the α and β angles to accommodate a certain magnification could affect the dispersion.

The nominal dispersion is set by the grating spacing and the focal length of the focusing lens. The plot shown in Figure X shows the ideal dispersion of the blue channel optical design. The grating spacing is set using the linear distance (9.152 mm) between the minimum and maximum wavelengths and the focal length of the focusing lens. For the blue channel, the ruling density is 864 grooves/mm, a density well within standard practices of commercial vendors. The specification on grating efficiency was >60% over the bandpass for unpolarized light. The remaining light goes in other diffraction orders.

iii. **Focusing Lens**

The blue focusing lens assembly is a set of five lenses packaged together. The lens uses Ohara I-line material, as the materials are made for good UV transmission and lens material uniformity. It is not clear that the materials used in the focusing lens are flight-qualified, but they have passed some radiation tests on the ground.

iv. Of the major optical design issues to be considered, the three primary concerns are spot size (currently the figure of merit is ensquared energy in a given pixel) over the field of regard at all wavelengths, slit curvature (i.e. distortion) and ease of fabrication and alignment (the back focus distance being a big concern). A self-imposed requirement was that the distance between the back of the lens housing and the location of the active surface of the detector, at best focus, had to be ~1 mm or greater.

The design of this lens assembly had to be concerned with 2 major aspects: the incoming beam size was ~50 mm and the f/no was f/1.5. A "fast" or small f/no usually implies very little back focus (the distance between the lens barrel or last lens and the detector) and steeply curved lens shapes. In the current design, all shapes are spherical. In the future, aspheric shapes should be investigated as it offers the potential of reducing the number of lenses required.

For fabrication, it was decided that the best approach for the IIP would be to specify a basic lens prescription to the vendor, without any tolerances, and an acceptable performance, in this case using rms wavefront error. The actual fabrication and alignment errors of each lens element were determined by the manufacturer. The manufacturer also was allowed to specify the AR coatings used on each surface; the only instruction to the vendor was to minimize the ghosting effect.

The resulting imaging performance is shown in Appendix A for the blue channel; only the performance near the ends and center of the bandpass are shown, but the performance at other wavelengths are very similar.

b. Red Channel spectrograph

i. Dichroic beamsplitter – the original transmission and reflectivity specifications for the red channel dichroic are shown in Table 3.

Table 3. Optical Specifications for red channel dichroic:
1. Average % Reflectance > 90% (Between 570-885 nm)
2. Average % Transmittance > 95% (Between 905-2160 nm)
3. Transition width from 5 to 95% average transmission: 20 nm on either side of pass band
4. AR coating on rear surface (transmitted output side)

The red band dichroic reflection and transmission curves are shown in a separate document[4], along with the figure specifications The figure specifications were determined by characteristics of good fabrication practices. Nominally the dichroic is flat, with no wedge between the front and rear surfaces, since ray tracing indicated that the wedge angle made no

difference on light that reflected off the rear surface and double passing through the dichroic getting into the blue focusing lens.

ii. Diffraction grating – the grating spacing was determined using Zemax optimization, with the light in 1st order used. The angle of diffraction was intentionally kept small, and using a larger angle of incidence. This configuration prohibited light at 0 order from entering the lens assembly. The gratings were chosen to be flat primarily to make manufacturing easier. An additional factor was that it was deemed very difficult to provide all the necessary aberration corrections with a single powered (non flat) surface.

Due to the broader spectral range of the red channel, the angles of incidence and diffraction, and assuming 1st order is used, cannot be the same as the blue channel. In the original design of the optics, a small angle of incidence (5°) was used, with a corresponding large diffraction angle at the center wavelength. This led into the discovery of the anamorphic magnification of a grating. The beam size after reflection at the grating is larger in the plane parallel to the grooves than the plan perpendicular to the grooves by the ratio cos(angle of incidence)/cos(angle of diffraction). This makes the exiting beam either larger (if the angle of diffraction is large) or smaller (angle of diffraction is small) than the beam perpendicular to the rulings. A larger beam causes a reduction in spectral resolving power. To address this problem, a grating with a small angle of diffraction is needed. The original design of the red channel spectrograph had a large angle of diffraction, but was modified to use a large angle of incidence and small angle of diffraction after test results showed a images with a large slit width on the detector.

Holographic gratings were examined, but no vendors could be found who would produce ORCA compatible gratings in a reasonable time for an amount affordable under the IIP. Therefore a conventionally ruled grating was chosen.

Similar to the blue grating, the final ruling density needed was determined by optimization in Zemax, with the ruling density set to 702.5 grooves/mm, a density is well within standard practices of commercial vendors. The specification on efficiency was >60% over the bandpass for unpolarized light. The remaining light goes in other diffraction orders.

iii. **Focusing Lens** – the blue focusing lens assembly is a multielement (5) set of lenses. For the red lens, all the materials are Schott glass, using industry standard materials.

The design of this lens assembly had to be concerned with 2 major aspects: the incoming beam size was ~50 mm and had to be used at f/1.5. The fast number usually implies very little back focus (the distance between the lens

barrel or last lens and the detector) and steeply curved lens shapes. In the current design, all shapes are spherical. The surface of best image quality is slightly tilted with respect to the last lens surface.

It was decide that the best approach for the IIP would be to specify a basic lens prescription to the vendor, without any tolerances, and just specify the acceptable performance, in this case using rms wavefront error. The actual fabrication and alignment errors of each lens element were determined by the manufacturer. The manufacturer also was allowed to specify the AR coatings used on each surface; the only instruction to the vendor was to minimize the ghosting effect.

The imaging performance for the red channel is shown in Appendix B. Only performance for wavelengths near the ends and center of the bandpass are shown, but all others are very similar.

c. Optical MTF

The limitations of the optical MTF performance of ORCA are primarily geometrical aberrations. The important characteristic of ORCA to note, though, is that the system is pixel limited, from a spatial frequency point of view. It is the size of the superpixel (208 microns in the nominal design) that limits the spatial frequencies of interest to a very low value, <= 2.4 cycles/mm. The calculations are based on a formula in Schroeder's book[5].

Shown in Figure 26 are the optical MTF results for the blue channel. Figure 27 shows the MTF results for the red channel. For several different wavelengths across the full width of each band, the plot shows the MTF in both the cross track and long track directions. For a given wavelength, calculations of the MTF were made by averaging the MTF over the slit image at the center, edges, and corners of the image. This was done for the baseline optical design for each channel (i.e. no fabrication or alignment errors were included). When evaluated at the spatial frequency set by the superpixel size, all the results for the optical MTF for all wavelengths in both channels were greater than 0.95.

SWIR Optics

For the IIP, three SWIR bands centered at 1240 nm, 1645 nm, and 2130 nm were incorporated (Table 2). For reasons of simplicity, a decision was made to use three different imaging channels separated by dichroic beamsplitters and with narrowband filters in each of them. These bands used 16 InGaAs detector linear arrays in a TDI scheme. The detector pixel size is 200 microns by 200 microns, arranged in a 16x1 row. This means the slit image at the SWIR detectors should be 200 microns, compared to 208 microns in the spectrograph channels. Thus, the SWIR lenses should also produce a f/1.5 beam. The TDI factor in the SWIR arrays is 16, making the active area of the detectors 200 microns x (200x16) microns, or 0.200 x 3.200 mm. Each of the SWIR detectors is housed in its own

cooling system with a sapphire window with a thickness of 1 mm; this window must be accounted for in the optical design. It should be remembered that only the detector is cooled – not the optics or surrounding structure.

a. The optical design for the SWIR optics was intended to be the same for all three bands, if possible. The lens system needs to provide as high a throughput as feasible. We chose IR grade fused silica as the dichroic substrates (for manufacturing and cost reasons) and LAK9G15 as the lens material (high throughput, availability). During the design process, it was discovered that using an aspheric surface simplified the design by allowing some lens elements to be removed. The current design uses an elliptical conic constant on the convex surface of the first lens element; there are only two lens elements in the design.

b. The narrowband filters in each channel are tilted in their mounts by 2° to avoid ghost reflections hitting the active area of the detector. This refers to ghosts that reflect from the back side of the filter, travel to the front side, and then reflect again and travel the normal path to the detectors. The filters themselves are not wedged.

PUPILS

a. Entrance Pupil

Using an internal aperture stop means that the entrance pupil is virtual. For ORCA, the system entrance pupil is located behind the primary mirror (i.e. on the opposite side of the primary as the depolarizer). There is pupil wander on the primary mirror of about 2.4 mm over the field of view, the vast majority being in the spatial (cross track) direction.

The summary values for the entrance pupil are:
Pupil Location = 280 mm behind the primary mirror
Pupil Diameter = 89.4 mm

b. Exit Pupils

Table 4 lists the exit pupil diameters and positions for each of the bands. The positions are relative to the focal surface of the channel; a positive distance means a longer distance from the last optic.

	Diameter (mm)	Position (mm)
BLUE	4.4	6.2
RED	3.6	4.7
SWIR1	2.9	3.6
SWIR2	2.2	-7.4
SWIR3	2.0	3.3
SWIR4	1.9	-7.7
SWIR5	3.9	2.4
SWIR6	1.6	3.7

Stray Light

There were several items that needed to be considered in minimizing the effects of stray light in ORCA. Here stray light refers to both out of field stray light (light that reaches the detector from outside the nominal field of view) and in field stray light, including both scatter from the optics and additional grating orders that reach the detector.

To minimize out of field stray light, a baffle tube was placed around the telescope optics. The length of this tube should be long enough to cut off light near the edge of the FOV and is the distance from the front of the primary mirror to the end of the tube . For ORCA, a stray light analysis indicated that a length of at least 350 mm was needed. Because of mechanical constraints, i.e., the need to minimize mass and volume, this was the length selected. Figure 11 is a plot of power versus tube length.

The analysis also indicated that at least two vanes were to be placed along the length of the tube. These are circular rings with holes large enough to pass the beam representing the full FOV. The first vane prevents light from going through the opening in the tube without striking any optics. The second vane is near the primary mirror and serves a similar purpose. The second vane is placed above and slightly forward of the depolarizer, since it was necessary to place part of the depolarizer inside the baffle tube and part outside. See Figure 10 for a drawing of the telescope tube and associated parts.

Figure 10 Telescope Tube and vanes

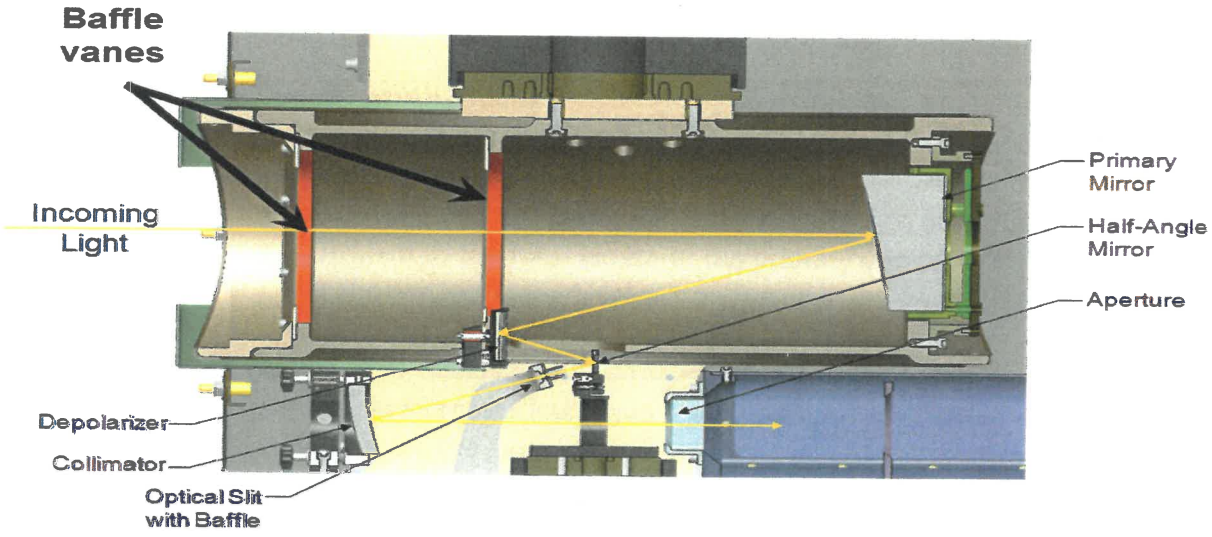

To handle out of field light rejection while the telescope is rotating, a separate rotating shield is used. The entire telescope assembly is then placed inside a fixed outer cover which has an aperture just large enough to pass the full field of regard (+/- 58 deg). Another, fixed cover was placed below the telescope tube and in front of the collimator to prevent light from entering the instrument from below the telescope tube.

There were two other out of field stray light techniques used including a baffle just in front of the slit that is attached to the slit mount (minimizes stray light from just outside the edge of the

FOV), and an internal stop located (minimizes light reflecting off any structural component falling on the detector (see Figure .

Ray tracing results indicated two other sources of stray light should not be a problem, i.e., reflections off the back side of the dichroics and additional grating orders. For these sources, stray light would not reach the detector, or have very minimal impact as the power would be down by ~10^{-7}.

In-field scattering

This has by far the biggest impact on image quality. The primary mirror is a dominant source of such scatter. A specification of 10 Angstroms RMS was specified for this optic making it a very good mirror, but data analysis shows that it still has an impact on stray light seen by the instrument.

The other sources are: 1) ghost reflections from the front surface of the depolarizer (~3% of the light is reflected), and the split images from going through the depolarizer (the s and p components have different optical paths through the crystal). The latter is dealt with by merging the two images into nearly a single image on the detector via the spectrograph lenses as discussed

Other possible contributors are ghosts from the lens systems in each spectrograph channel. The primary concern is a reflection from the detector surface back to the last lens surface which then gets reflected back to the detector. This would be almost in focus. Slight tilts in the best focus surface could be one way to minimize this affect and this is used in the current red channel design.

Figure 11 - Stray Light rejection as a function of off axis angle, for 2 different tube lengths

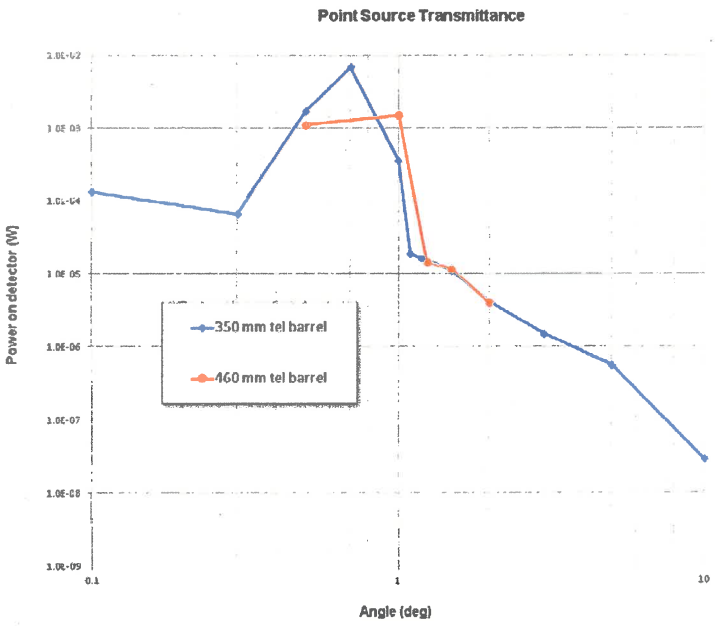

Optimizing for different altitudes

If an orbit other than the nominal height of 650 km is required, the ground resolution would change accordingly, such that the instrument field of view would remain constant. The aperture would scale by an amount needed to satisfy the SNR requirements. However, this scenario is unlikely as the science requirement for spatial resolution will most likely remain 1 km along the subsatellite ground track (this is the requirement of the PACE Science Definition Team).

a. Aperture considerations – An increase in the collecting aperture diameter affects the optics by requiring an increase in the off-axis distance of the primary mirror. This increases the off-axis aberrations, increasing the workload on the camera lens system and requiring a wider slit in the long track direction. Decreasing the altitude has the reverse effect (to some extent). The alternative is to accept some vignetting at different fields of view.

b. Telescope Focal Length considerations

The important trade off regarding the telescope focal length is the length vs. f/no. Keeping the f/no the same allows minimum changes in the aft optics at the expense of a longer (and therefore heavier) mass for the telescope subassembly (including the baffle tube surrounding the primary mirror). Keeping the f/no the same is recommended to minimize impacts in the spectrograph portion of the instrument. The variation of focal length scales linearly with the aperture diameter.

There are 3 points worth making:

1) Generally, the overall size of the telescope would linearly scale directly with the primary mirror diameter.
2) Both the depolarizer and half angle mirror are required to be mounted in a distance equivalent to the focal length of the primary mirror, relative to the primary. For shorter focal length telescopes (used in lower altitude designs), this packaging constraint could cause the telescope design to become more problematic.
3) The size of the slit increases linearly in both directions with telescope focal length, which causes the amount of demagnification of the spectrograph optics to increase (unless the detector pixel size increases as well)

c. IFOV considerations

Changing the altitude and keeping the ground footprint the same size (1 km nominal), causes the IFOV seen by the detector to change almost linearly (within the range of moderate changes in altitude). In this case, decreasing the altitude causes more problems in the optical design because the IFOV is increased, so the beam clearance around the optics is decreased – i.e. the packaging becomes more difficult.

d. Impact on spectrograph optics

Impacts on the spectrograph optics should be minimized. It is very possible that the current optics are either undersized or oversized for other altitude options. Undersizing is a workable situation, oversizing can be problematic. The latter is particularly true for the camera lenses in the spectrographs because of some steeply curved lens surfaces. The larger the aperture on these lenses the harder it is to find a design solution that can be built.

APPENDICES

The appendices that follow show specific details of the baseline optical design, including lens drawings, spot diagrams, encircled energy, and stray light analysis results.

Appendix 1 Lens Drawings

Figure 12a Lens Drawing of Full System (Top View)

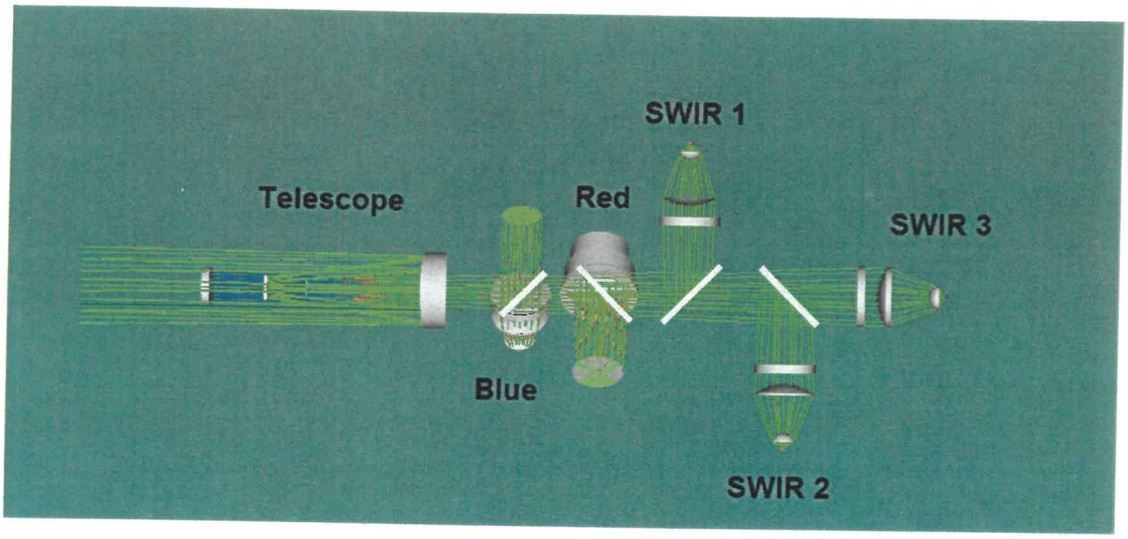

Figure 12b Lens Drawing of Full System (Side View)

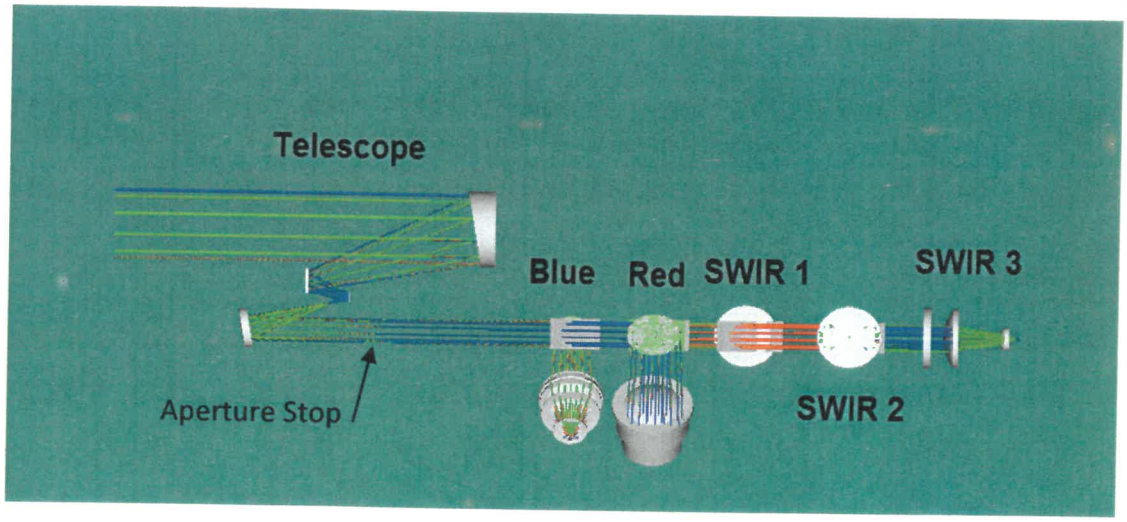

Figure 13 BLUE CHANNEL RAY TRACE (YZ VIEW)

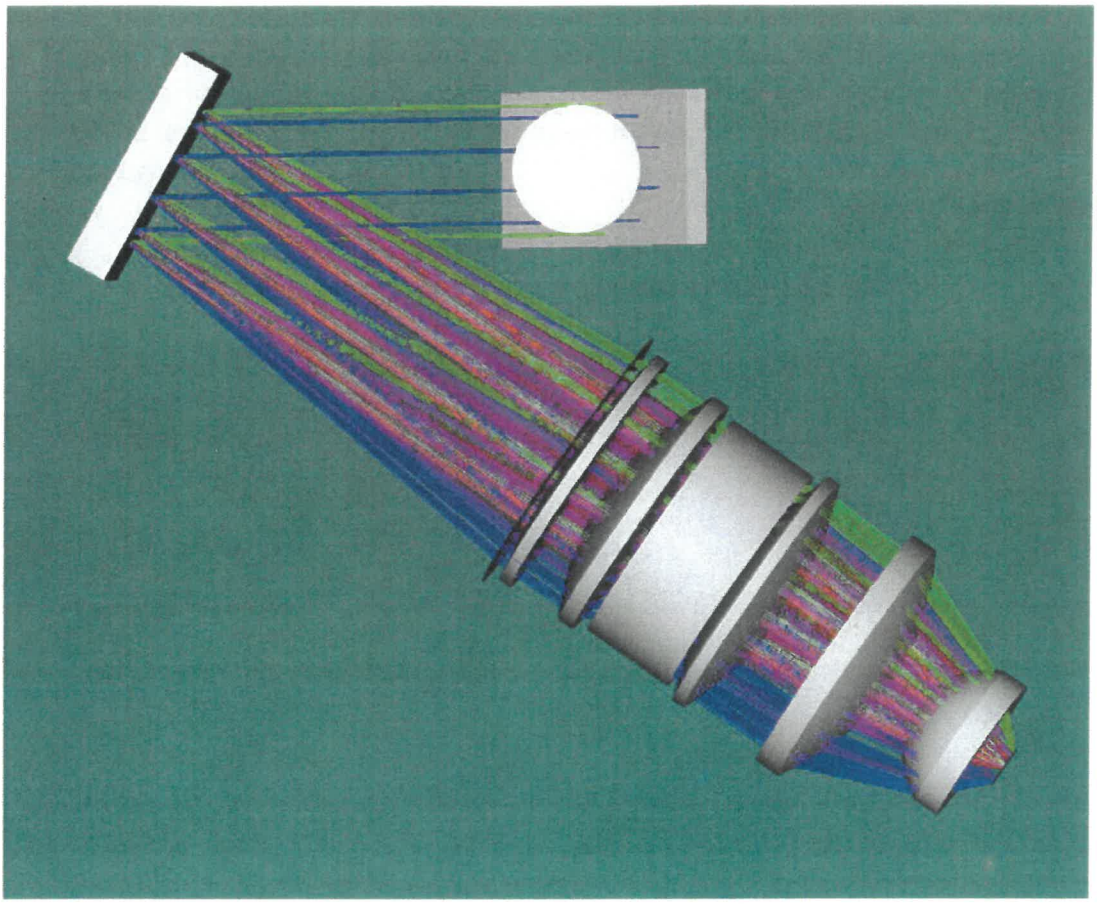

Figure 14 - RED CHANNEL RAY TRACE (XY VIEW)

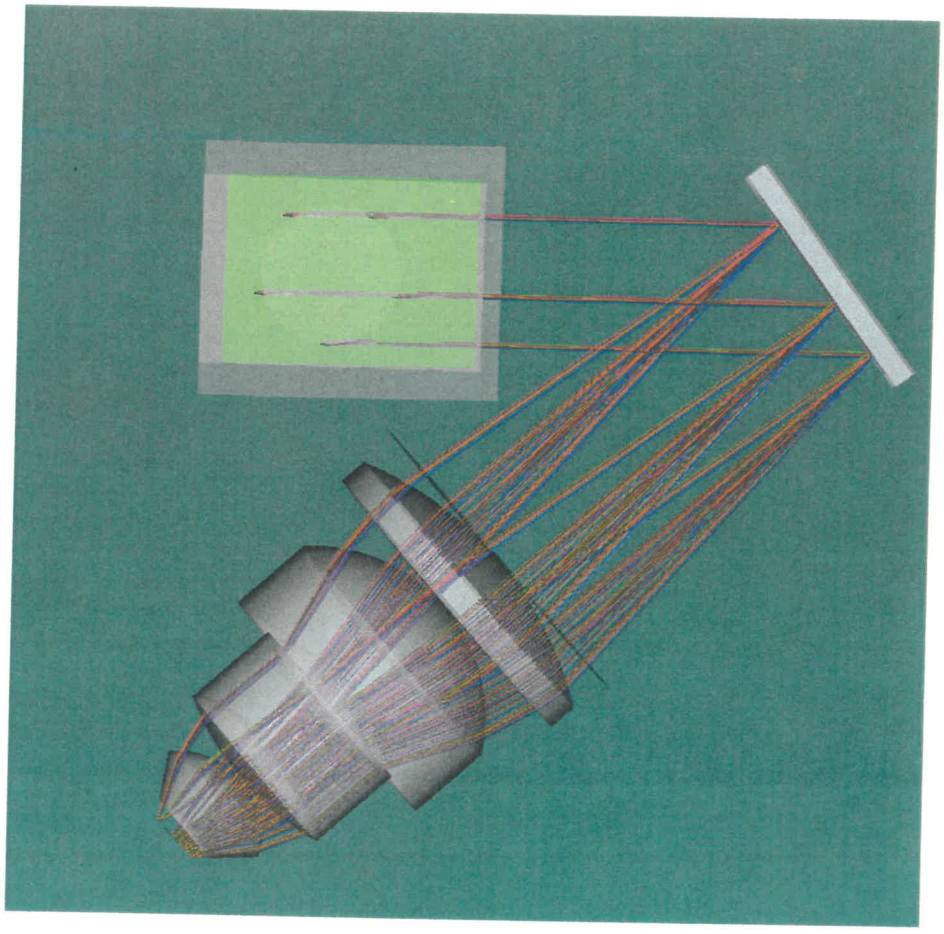

Figure 15 - SWIR CHANNELS RAY TRACE (YZ VIEW)

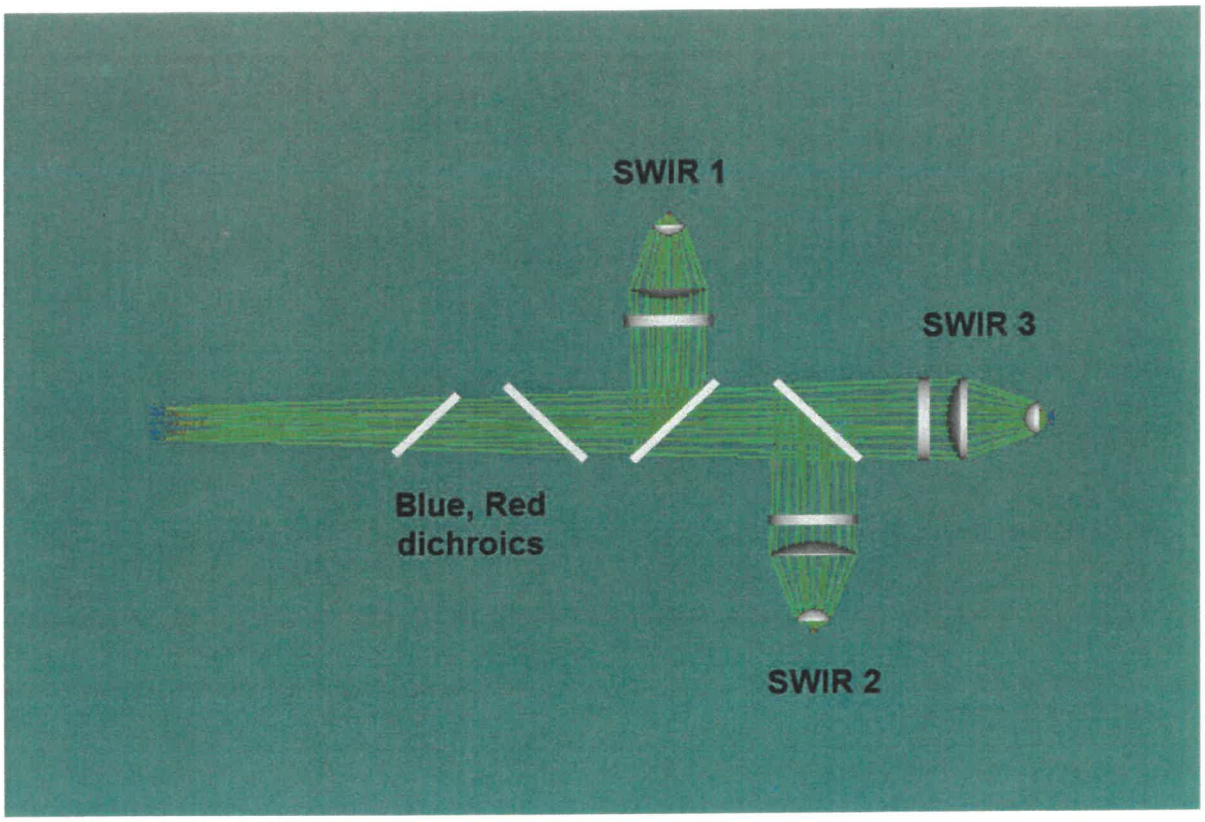

Appendix 2. SPOT DIAGRAMS AT SLIT (CONVENTIONAL RAY TRACE)

The slit is located at the optimum focus of the primary mirror. Because of the off-axis nature of the primary mirror, the slit image surface is slightly tilted with respect to the chief ray. The slit was sized so that there is no vignetting over the field of view corresponding to a 1 km ground spot. Figure 15 shows the spot diagrams at the center and corners of the field of view.

Figure 15 - Images at Slit (standard ray tracing)

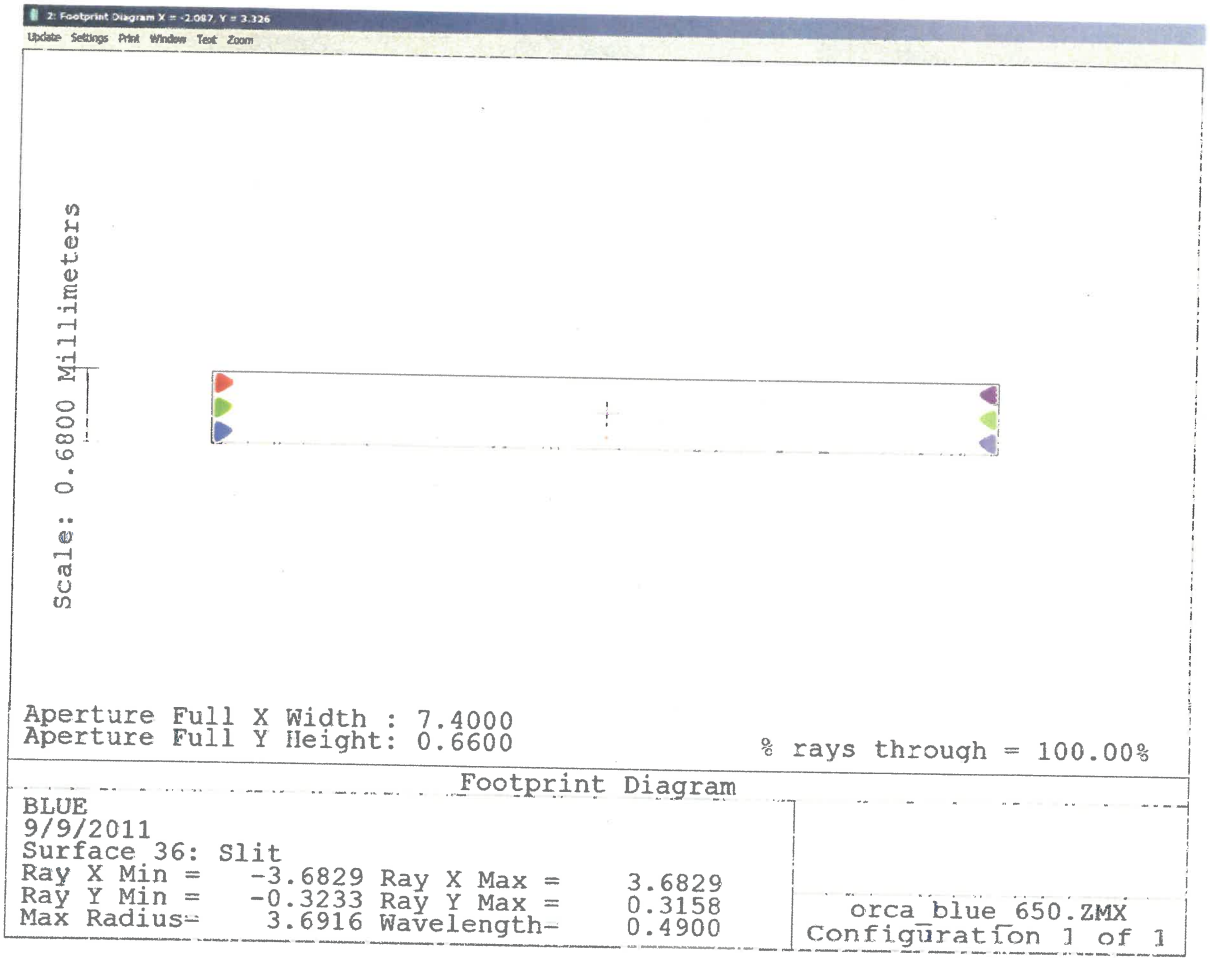

Appendix 3. BLUE CHANNEL SPOT DIAGRAMS AT DETECTOR

The goal of the optical design was to get rms spot diameters <= 2 pixels in diameter. Diffraction effects are neglible in this system – a typical Airy disk is ~3-4 microns in diameter. The geometric spots show the general behavior of the images – the most important criteria is ensquared energy shown in section XIV.

Figure 13 - Spot diagrams at λ = 350 nm

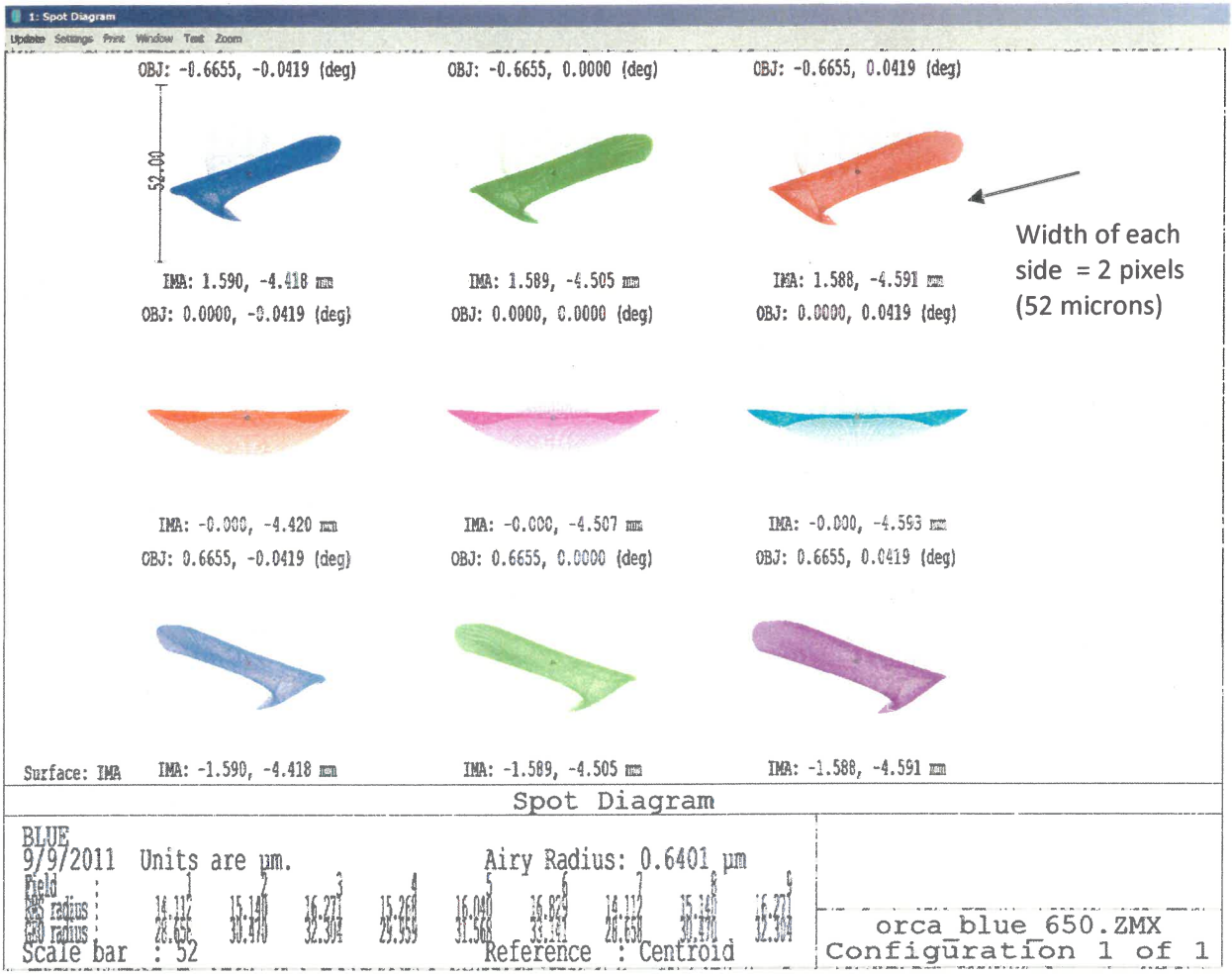

Figure 14 - Spot Diagrams at λ = 490 nm

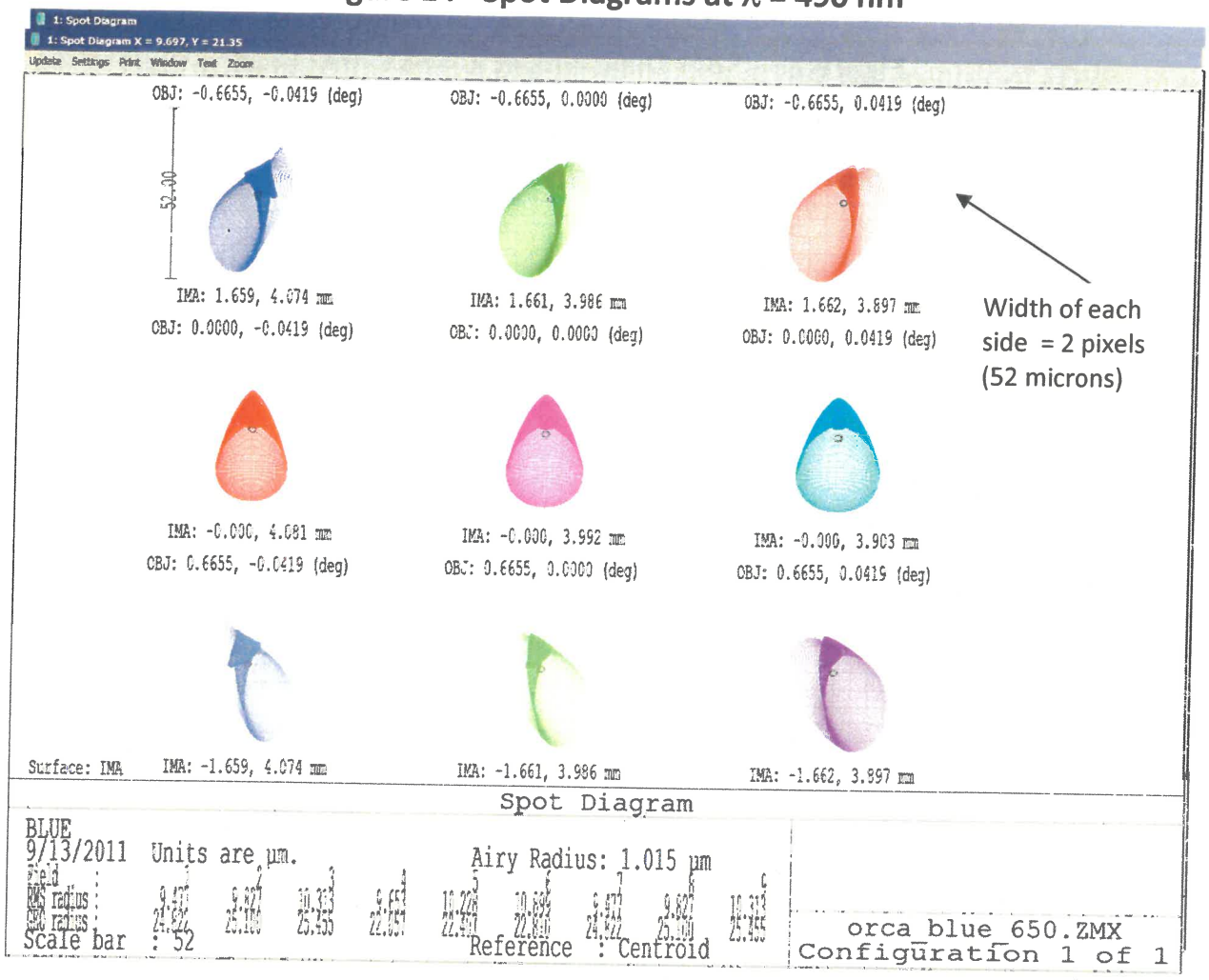

Figure 15 - Spot Diagrams at λ = 555 nm

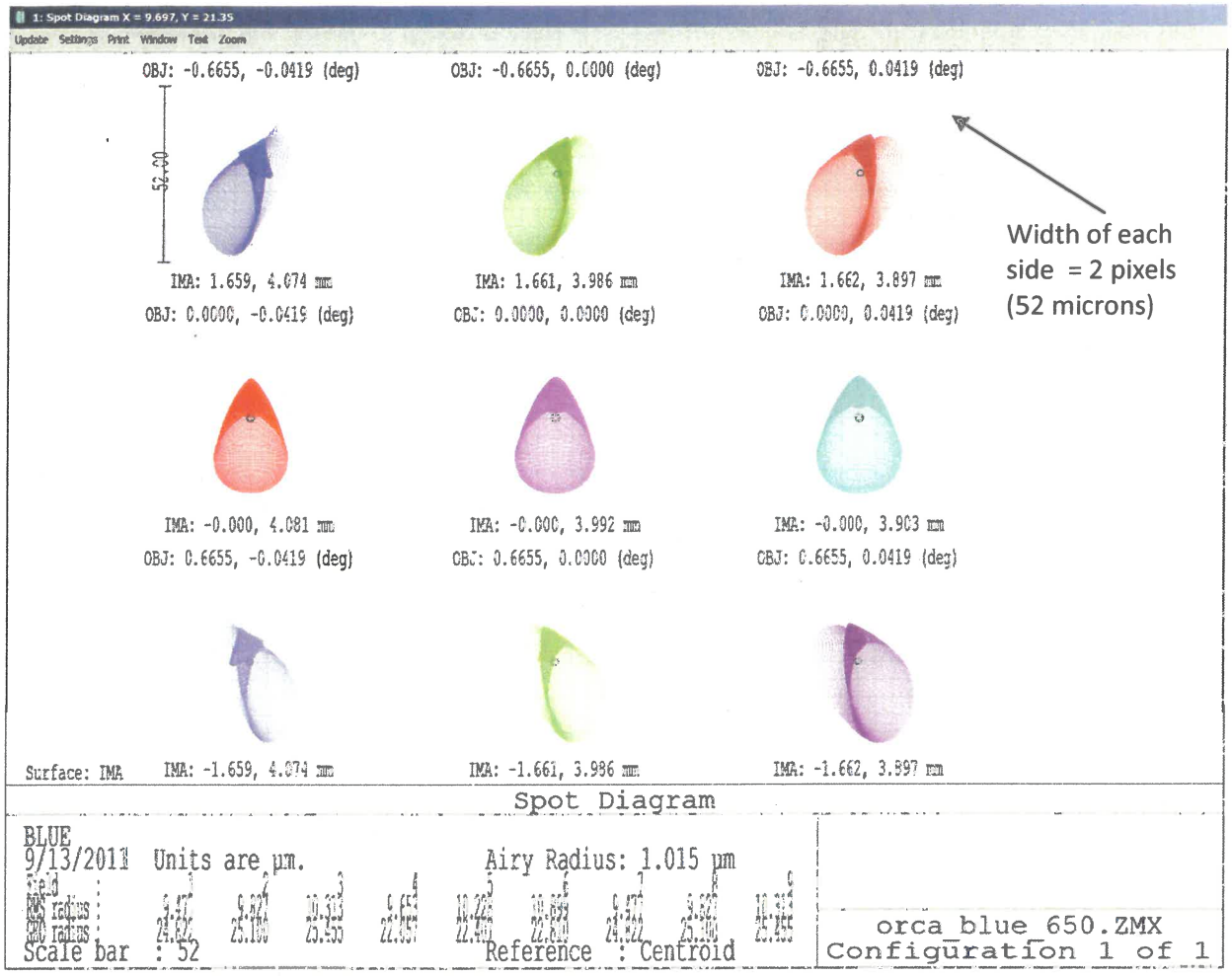

Appendix 4. BLUE CHANNEL ENSQUARED ENERGY AT DETECTOR

Figure 16- Blue Channel, Ensquared Energy at 490 nm, center of FOV

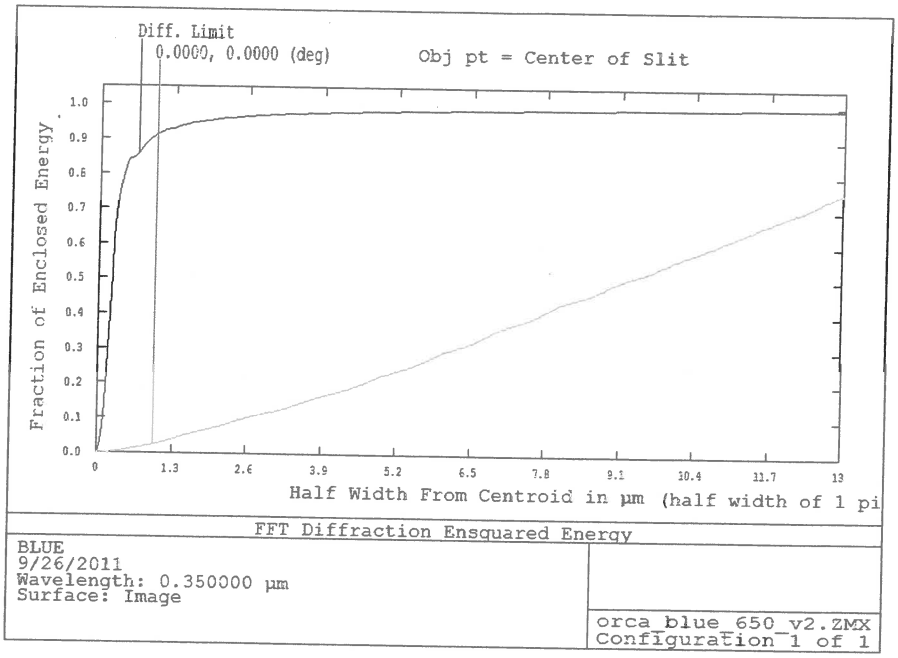

Figure 17- Blue Channel, Ensquared Energy at 490 nm, center of FOV

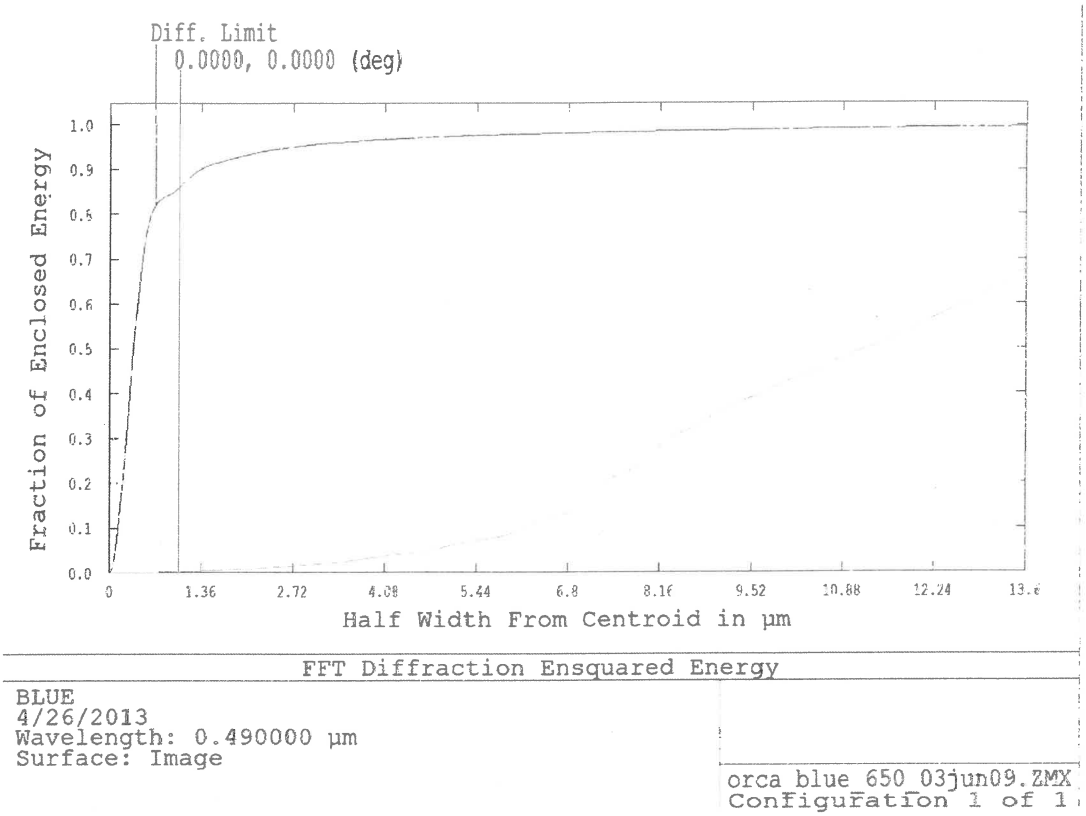

Figure 18- Blue Channel, Ensquared Energy at 555 nm, center of FOV

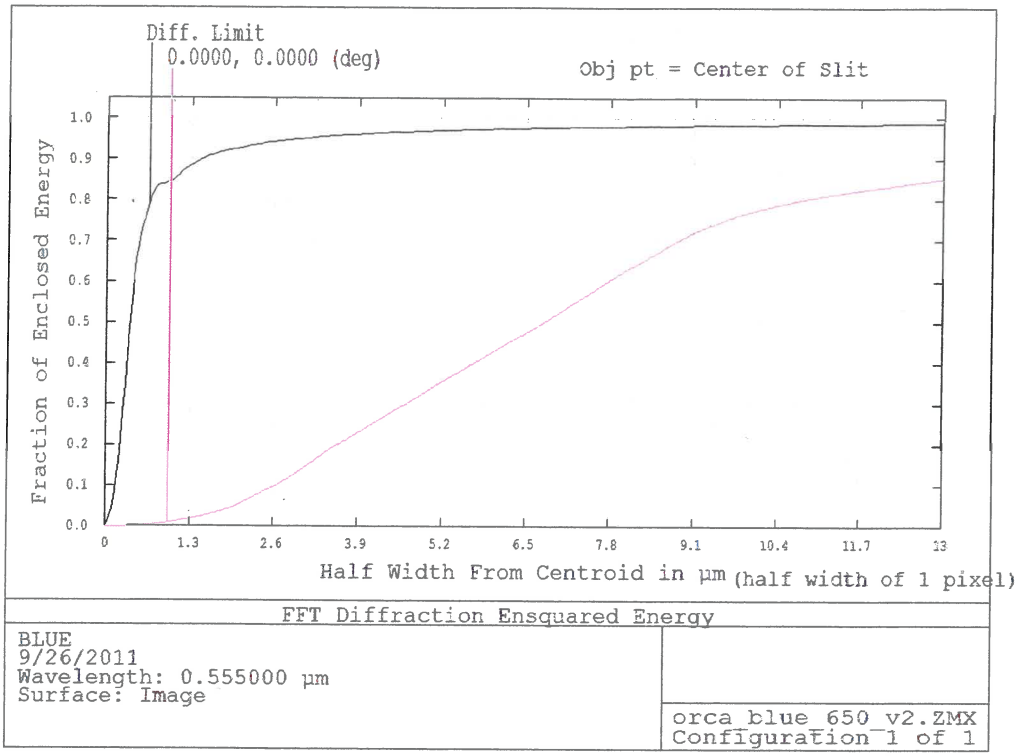

Appendix 5. RED CHANNEL SPOT DIAGRAMS AT DETECTOR (Each spot represents a different position across the slit)

Figure 19 - Red Channel spot diagrams at 617 nm

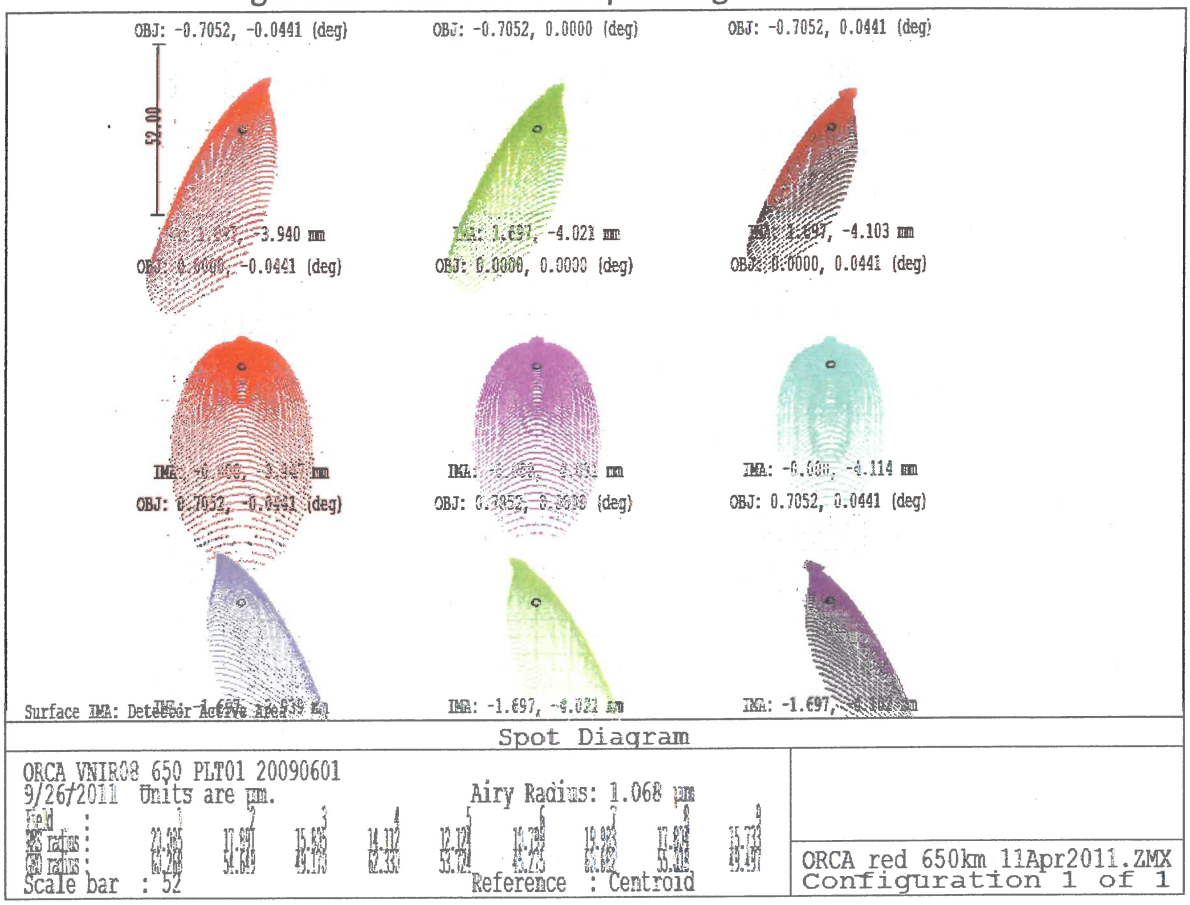

Figure 20 - Red Channel spot diagrams at 738 nm

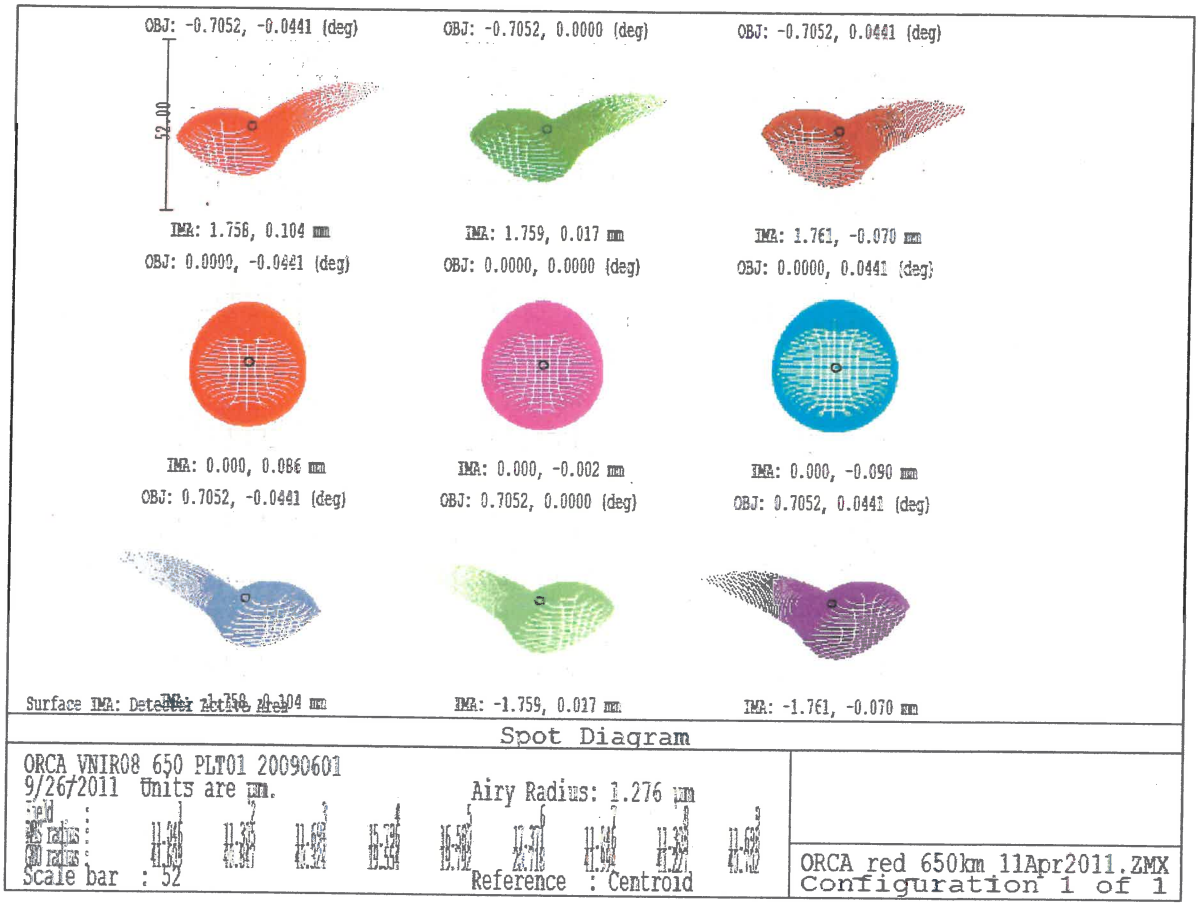

Figure 21 - Red Channel spot diagrams at 865 nm

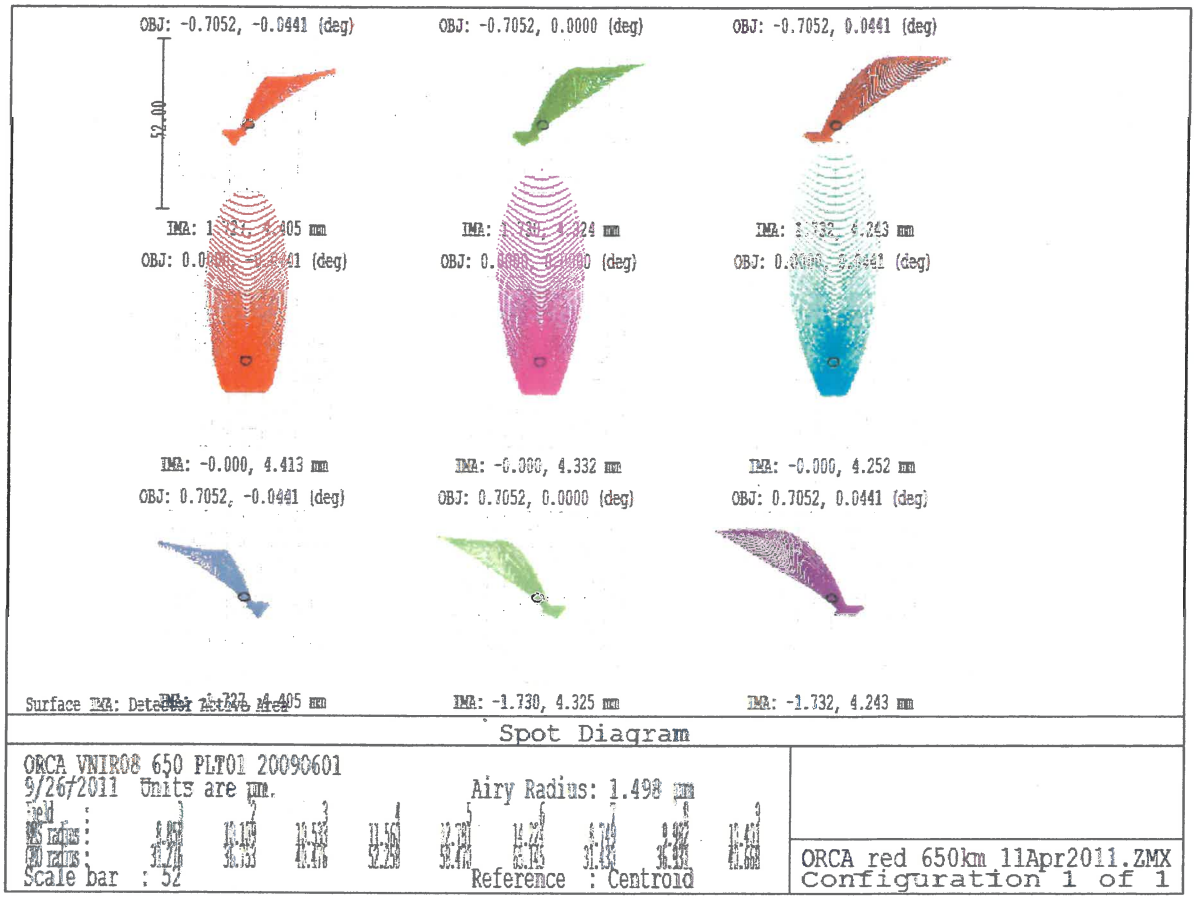

Appendix 6. RED CHANNEL ENSQUARED ENERGY AT DETECTOR

Figure 22 - Ensquared Energy in 1 pixel at 617 nm

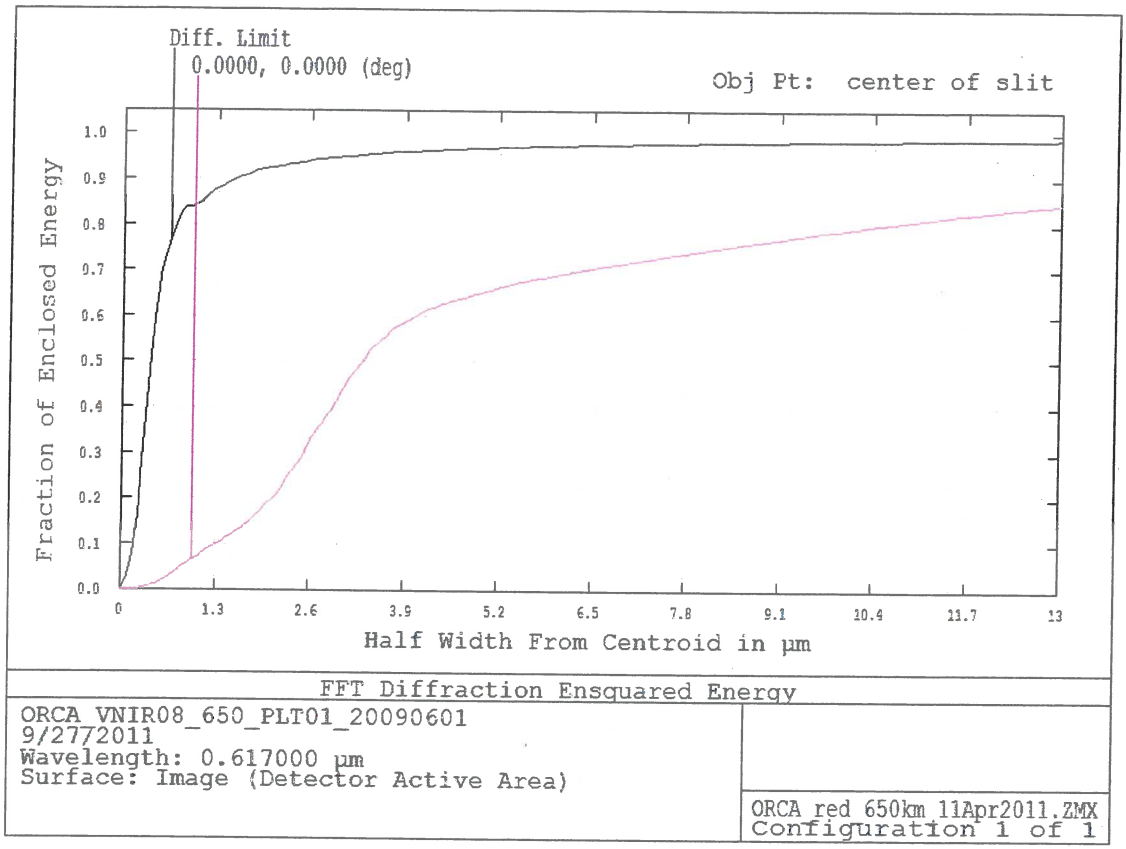

Figure 23 - Ensquared Energy in 1 pixel at 780 nm

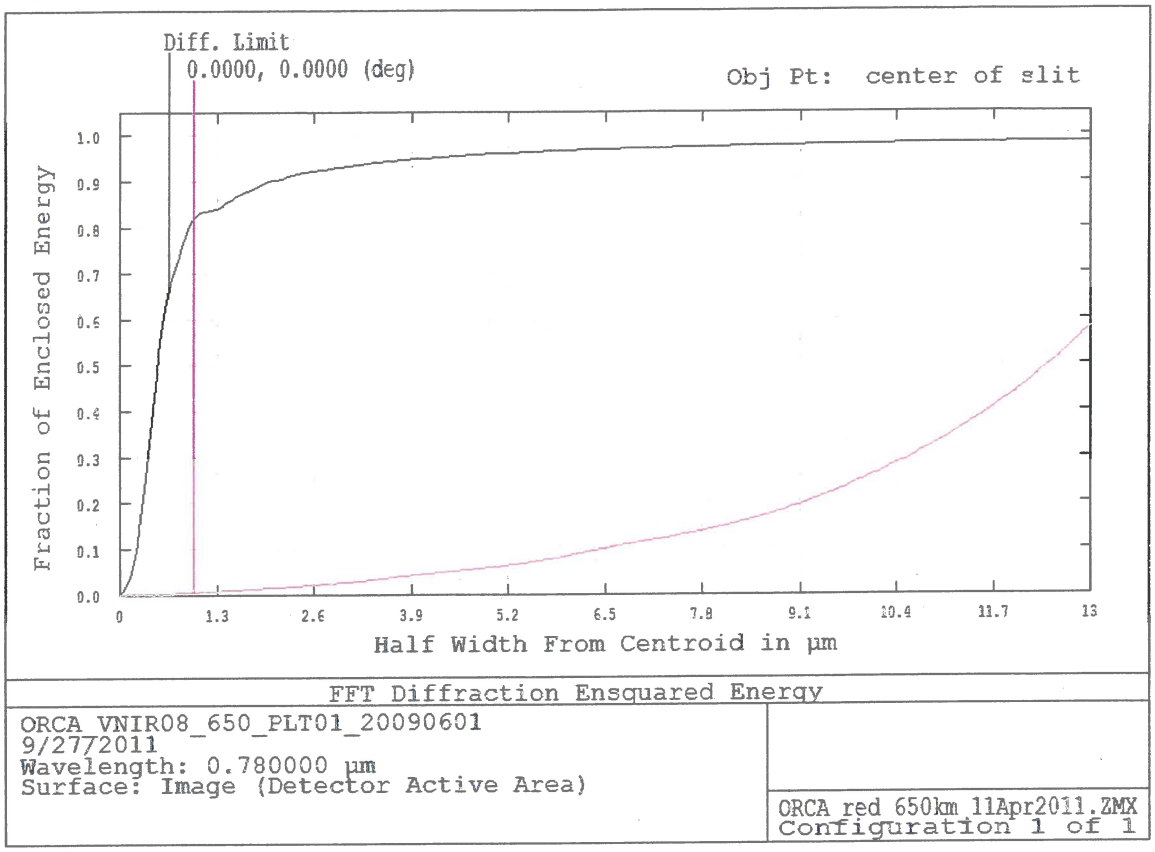

Figure 24 - Ensquared Energy in 1 pixel at 865 nm

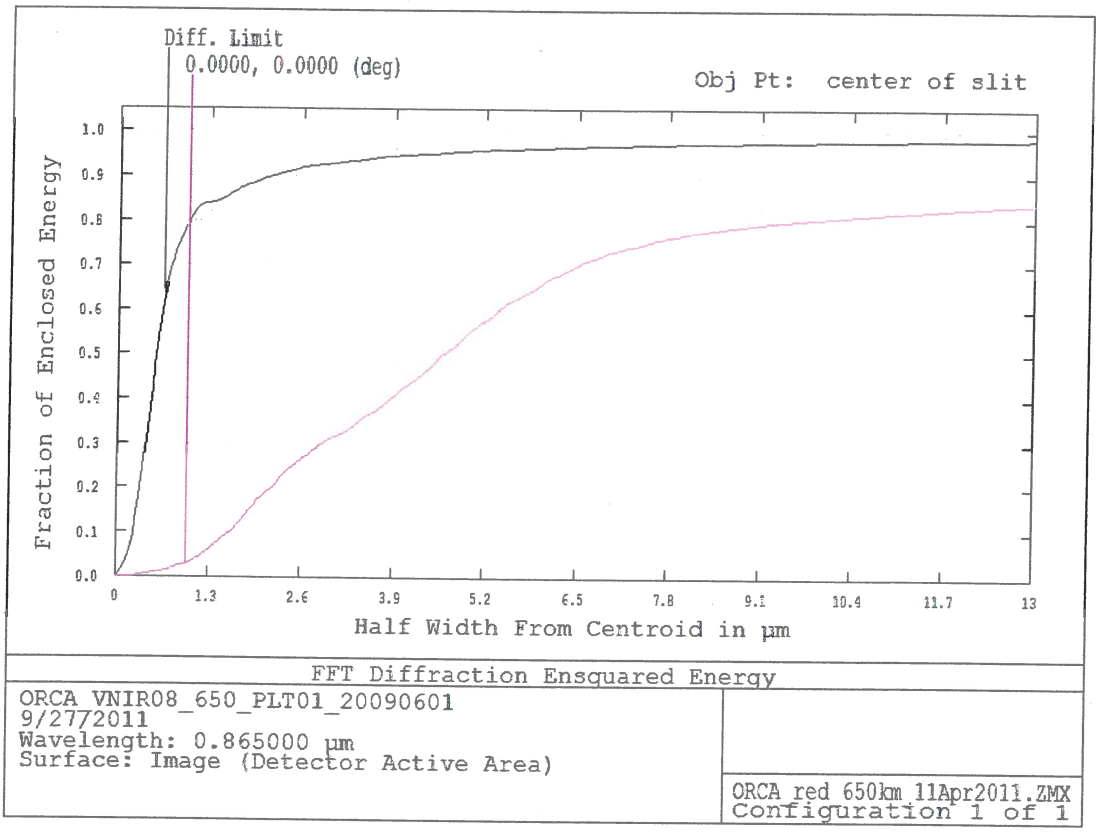

Appendix 7. EFFECT ON SPOTS DUE TO IMAGE SPLITTING CAUSED BY POLARIZATION

Figure 25- Images at Slit showing split images due to polarization

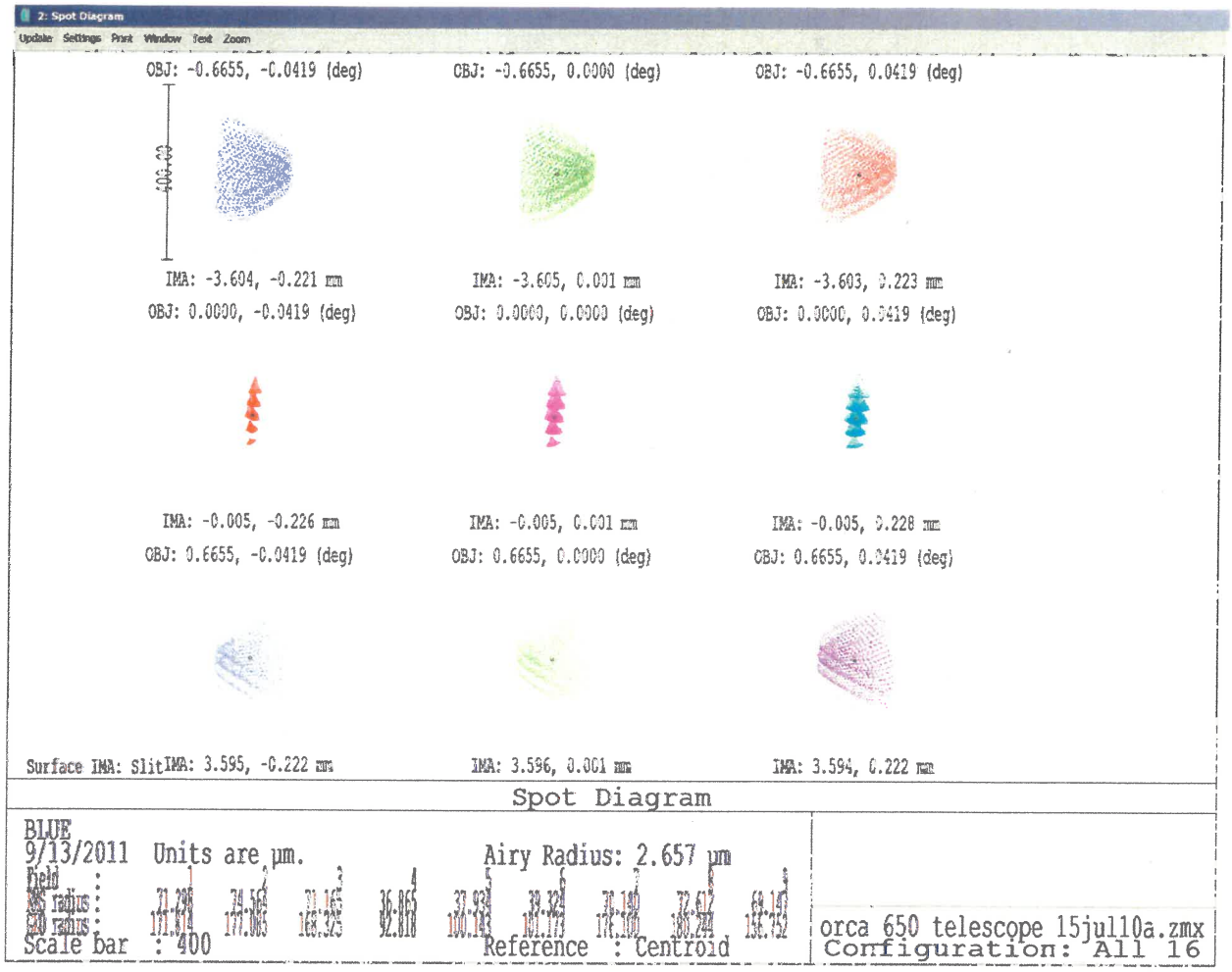

Appendix 8. OPTICAL MTF

Figure 26 - Optical MTF of Blue Channel

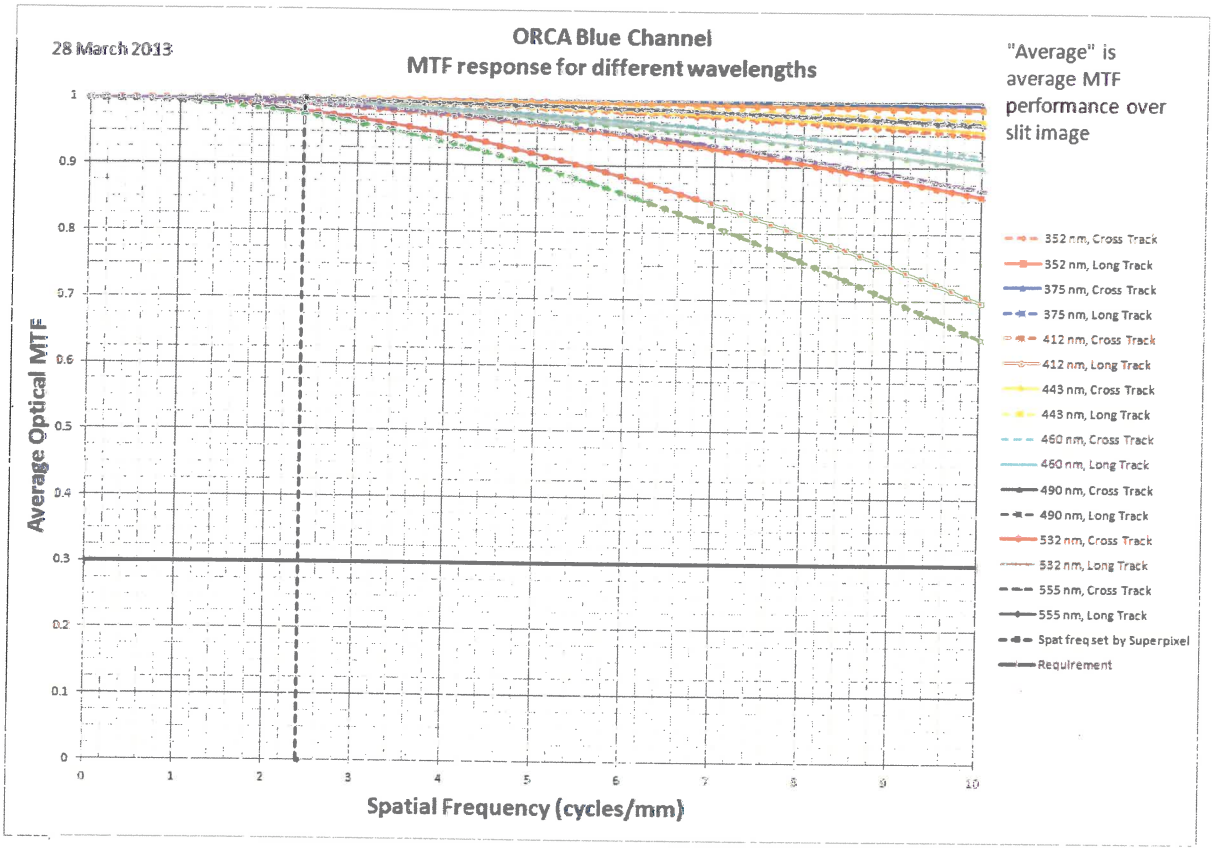

Figure 27 Optical MTF of Red channel

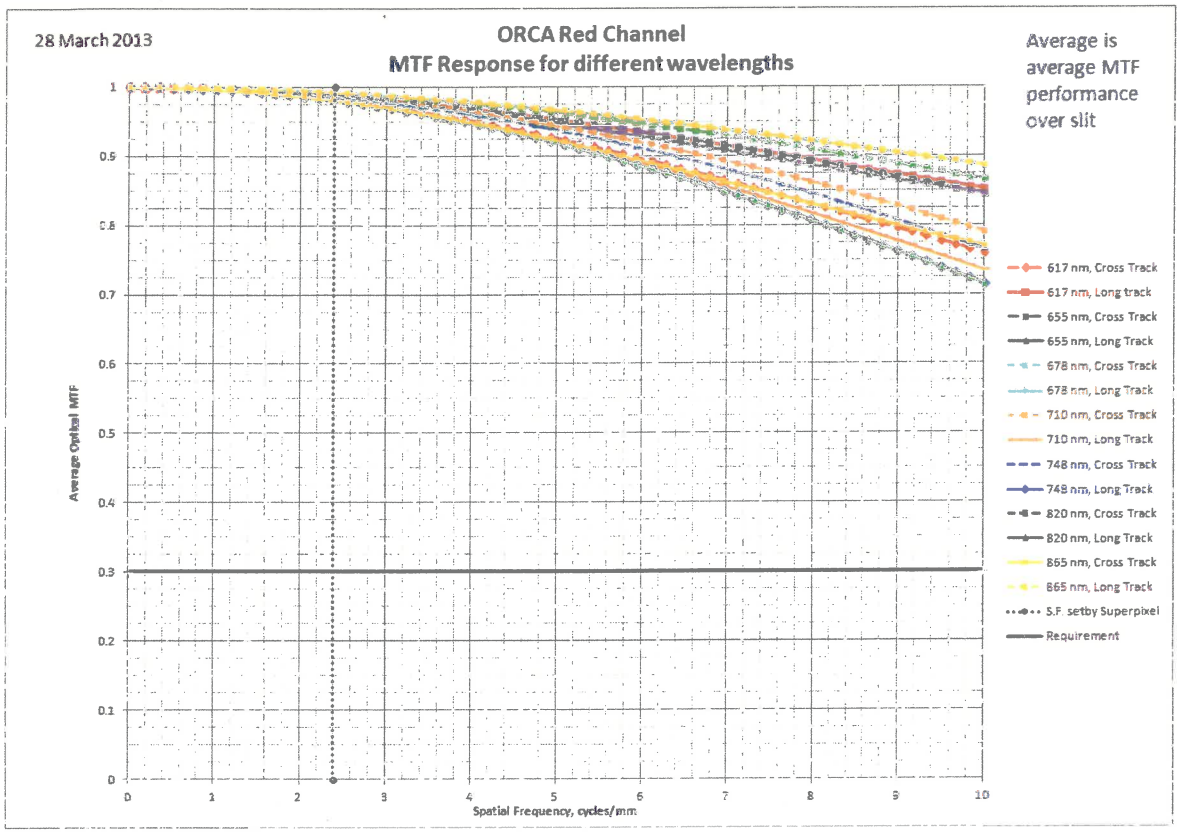

References

1. McClain, C., M. Behrenfeld, M. Wilson, B. Monosmith, M. Quijada, G. Meister, P. Shu, L. Sparr, P. Thompson, K. Blumenstock, A. Holmes, B. Martin, and F. Patt, The Ocean Radiometer for Carbon Assessment (ORCA): Development history within an advanced ocean mission concept, science objectives, design rationale, and sensor prototype description, NASA/TM-2012-215894, Goddard Space Flight Center, 55 pp., 2012.

2. Monosmith, B., and C. McClain, Ocean Radiometer for Carbon Assessment (ORCA) system design and radiometric performance analysis, NASA/TM-2012-215896, Goddard Space Flight Center, 35 pp., 2012.

3. Meister, G., C. McClain, Z. Ahmad, S. W. Bailey, R. A. Barnes, S. Brown, G. E. Eplee, B. Franz, A. Holmes, W. B. Monosmith, F. S. Patt, R. P. Stumpf, K. R. Turpie, and P. J. Werdell, Requirements for an Advanced Ocean Radiometer, NASA T/M-2011-215883, NASA Goddard Space Flight Center, Greenbelt, Maryland, 37 pp., 2011.

4. Quidaja, M., M. Wilson, T. Madison, P. Petrone, and C. McClain, Optical component performance for the Ocean Radiometer for Carbon Assessment (ORCA), NASA/TM-2012-215895, Goddard Space Flight Center, 43 pp., 2012.

5. McClain, C. R., G. C. Feldman, and S. B. Hooker, An overview of the SeaWiFS Project and strategies for producing a climate research quality global ocean bio-optical time series, Deep-Sea Res. II, 51(1-3), 5-42, 2004.

6. Gregg, W. W. and F. S. Patt, Assessment of tilt capability for spaceborne ocean color sensors, IEEE Trans. Geosci. and Remote Sens., 32(4), 866-877, 1994.

7. Schroeder, Daniel J. , Astronomical Optics, 2nd Edition, Academic Press, 2000, p. 428.